U.PORTO
INSTITUTO DE CIÊNCIAS BIOMÉDICAS ABEL SALAZAR
UNIVERSIDADE DO PORTO

U.PORTO
FEUP FACULDADE DE ENGENHARIA
UNIVERSIDADE DO PORTO

DEVELOPMENT OF QUERCETIN BRAIN DELIVERY SYSTEMS FOR THE TREATMENT OF ALZHEIMER'S DISEASE

Rúben Gonçalo Rodrigues Pinheiro

Master Thesis for the degree in Master in Bioengineering
Specialization in Molecular Biotechnology

Supervisor: Doutora Salette Reis

Co-supervisor: Doutora Ana Rute Neves

02 October 2017

- This page was intentionally left in blank –

ABSTRACT

Quercetin is a flavonol present in many vegetables and fruits with many beneficial effects such as anti-cancer, anti-inflammatory, anti-oxidant and neuroprotection action. However, due to its lipophilicity, low water solubility, and extensive metabolism, quercetin presents poor bioavailability and cannot be used efficiently for diseases prevention or treatment. In this context, nanotechnology can help to overcome this problem by encapsulating quercetin inside nanoparticles to increase its bioavailability and potentiate its efficacy by directing to a specific target of interest.

The main goal of this work was the development of quercetin-loaded lipid nanoparticles (SLN and NLC) functionalized with transferrin and RVG29 peptide for enhancing the bioavailability of quercetin, promoting its site-specific delivery through the blood-brain barrier (BBB) into the brain with the utmost purpose of treating or preventing Alzheimer's disease. In fact, transferrin and nicotinic acetylcholine receptors are highly expressed on BBB, potentiating receptor-mediated transcytosis of transferrin- and RVG29-coated nanoparticles, respectively, to the brain.

Functionalization has been confirmed using nuclear magnetic resonance and Fourier transform infrared spectroscopies. All nanoparticles appeared to have a spherical and uniform morphology with smooth surfaces, analyzed by transmission electron microscopy. Transferrin and RVG29 nanoparticles were capable of encapsulating around 80-90% of quercetin and this value remained almost unchanged over 3 months of stability study. The size of both modified nanoparticles was between 150 and 250 nm and zeta potential was around -30 mV, which is a good indicator of formulation stability. Photostability study showed that free quercetin was degraded (55%) after 6 hours of UV light exposure, but lipid nanoparticles protected the compound against photodegradation.

The cytotoxicity of nanoparticles was tested by lactate dehydrogenase assay in hCMEC/D3 cell line, a model of human BBB. This assay showed almost no cytotoxicity even for the highest concentration tested. The BBB permeability of nanoparticles across hCMEC/D3 cells monolayer was tested using Transwell devices. The results showed that RVG29 nanoparticles can pass through the monolayer more efficiently than transferrin-functionalized or non-functionalized nanoparticles, probably due to the active expression of nicotinic acetylcholine receptors on brain endothelial cells. In order to test the efficacy of the developed nanoparticles for preventing Aβ(1-42) peptide fibrillation in Alzheimer's disease, a ThT binding assay was performed. Almost all

quercetin-loaded nanoparticles were able to inhibit fibrils formation, but especially transferrin- and RVG29-functionalized NLC may have a greater potential to be used in Alzheimer's prevention or therapy.

RESUMO

A quercetina é um flavonóide presente em muitas frutas e vegetais, com efeitos benéficos para a saúde, nomeadamente, propriedades anti-cancerígenas, antioxidantes e anti-inflamatórias, e ainda um efeito neuroprotetor. No entanto, devido à sua lipofilicidade, baixa solubilidade em água e extenso metabolismo, a quercetina apresenta baixa biodisponibilidade, não podendo ser utilizada de forma eficiente para a prevenção ou o tratamento de doenças. Neste contexto, a nanotecnologia pode ajudar a ultrapassar esse problema através da encapsulação da quercetina dentro de nanopartículas para aumentar a sua biodisponibilidade e potenciar a sua eficácia, direcionando-a para um alvo específico de interesse.

Neste trabalho, pensando numa abordagem para o cérebro, foram usadas nanopartículas lipídicas (SLN e NLC) funcionalizadas com Transferrina e RVG29, com intuito de as direcionar especificamente para o cérebro e, desta forma, a quercetina poder exercer o seu efeito neuroprotetor na prevenção ou tratamento da doença de Alzheimer. De facto, o receptor de transferrina e o receptor nicotínico da acetilcolina estão altamente expressos na barreira hematoencefálica (BHE), potenciando a transcitose mediada por receptores de nanopartículas revestidas com transferrina e RVG29, respectivamente, para o cérebro.

As funcionalizações com estes ligandos foram confirmadas utilizando as técnicas de espectroscopia por ressonância magnética nuclear e espectroscopia de infravermelho. Para além disso, a microscopia electrónica de transmissão permitiu ver que as partículas apresentavam uma morfologia esférica e uniforme. O tamanho medido por dispersão dinâmica da luz ficou compreendido entre os 150 e 250 nanómetros o que é adequado para atravessar a BHE. Por sua vez, os valores de potencial zeta rondaram os -30 mV o que garante a estabilidade das formulações. A taxa de encapsulação obtida foi alta, por volta dos 80-90%, mantendo-se estável ao longo de três meses de estudo. Quanto ao estudo da fotoestabilidade, foi possível observar que a quercetina encapsulada era protegida da degradação exercida pela radiação UV, contrariamente ao que se passava com a quercetina na forma livre que sofreu uma fotodegradação na ordem dos 55% ao fim de 6 horas de exposição.

Após esta etapa de caracterização, foram feitos estudos de citotoxicidade usando o ensaio da quantificação da enzima lactato desidrogenase, num modelo *in vitro* da barreira hematoencefálica composto pela linha celular hCMEC/D3. Os resultados mostraram que as partículas não induzem toxicidade, mesmo para as concentrações

mais altas estudadas. Foram ainda feitos estudos de permeabilidade usando uma monocamada de células hCMEC/D3 num ensaio feito com dispositivos Transwell, para testar a capacidade de permeação das nanopartículas através da BHE. As nanopartículas funcionalizadas com RVG29 foram as mais eficientes no aumento da permeabilidade através da barreira de células, tirando partido da presença dos receptores nicotínicos da acetilcolina presentes nas células endoteliais do cérebro. Por fim, para aferir o potencial terapêutico/preventivo destes nanosistemas, foi usado um modelo *in vitro* da doença de Alzheimer com o péptido Aβ(1-42). Os resultados mostraram que quase todas as nanopartículas carregadas com quercetina foram capazes de inibir a agregação do péptido, especialmente as partículas NLC funcionalizadas com transferrina ou RVG29, o que abre excelentes perspectivas para esta abordagem poder ser futuramente pensada como uma estratégia preventiva ou mesmo terapêutica da doença de Alzheimer.

ACKNOWLEDGMENTS

I am profoundly grateful to professor Salette Reis for giving me the opportunity to work in her research team and for all her kindness and comprehension in more difficult times.

I would like to thank to Dr. Ana Rute Neves for her guidance during these two semesters, for all the opportunities she has giving me, all her patience to listen to my concerns and all the encouragement.

I would like to thank to Andreia Granja for helping me with some of my experimental work, particularly for teaching me all about cells. Thanks for the support, good vibrations and all the hours that you spent with me in the lab.

I am deeply grateful to Alexandre Vieira for his kindness and support in some difficult stages of this work.

I would also want to thank Claudia, Joana and Pris for helping me to solve some pratical problems.

- This page was intentionally left in blank –

TABLE OF CONTENTS

ABBREVIATIONS AND SYMBOLS

DLS	Dynamic light scattering
EE	Encapsulation Efficiency
LDH	Lactate Dehydrogenase
ROS	Reactive Oxygen Species
SLN	Solid Lipid Nanoparticles
TEM	Transmission Electron Microscopy
CoA	Coenzyme A
IUPAC	International Union of Pure and Applied Chemistry
LUMO	Lowest unoccupied molecular orbital
HOMO	Highest unoccupied molecular orbital
UVA	Ultraviolet A
UVB	Ultraviolet B
COMT	Catechol-O-methyltransferase
AhR	Aryl hydrocarbon receptor
PAH	Polycyclic aromatic hydrocarbon
HAH	Halogenated aromatic hydrocarbon
CYP1A1	Cytochromes P450, family 1, subfamily A, polypeptide 1
CYP1A2	Cytochromes P450, family 1, subfamily A, polypeptide 2
CYP1B1	Cytochromes P450, family 1, subfamily B, polypeptide 1
DR5	Death receptor 5
TRAIL	NF-related apoptosis-inducing ligand
NF-kB	Factor nuclear kappa B
RVG-29	Rabie virus glycoprotein
DLS	Dynamic light scattering
BBB	Blood brain barrier
MNPs	Magnetic nanoparticles
PEG	Polyethylene glycol
PLGA	Poly(lactic- co-glycolic acid
PLA	Polylactic acid
ROS	Reactive Oxygen Species

MTT	Methylthiazolyldiphenyl-tetratozium Bromide
NO	Nitric Oxide
PCL	Polycaprolactone
MWCO	Molecular Weight Cut Off
NADH	Nicotinamide Adenine Dinucleotide – Hydrogen
CHD	Coronary heart diseases
u-PA	Urokinase-type plasminogen activator
t-PA	Tissue-type plasminogen activator
PAI-1	Plasminogen activator inhibitor
u-PAR	Urokinase-type plasminogen activator receptor
MCP-1	Monocyte chemoattractant protein 1
IL-1β	Interleukin 1 beta
PMA	Phorbol 12-myristate 13-acetate
IL-6	Interleukin 6
IL-8	Interleukin 8
eNOS	Endothelial nitric oxide synthase
PC	Phosphatidylcholine
EPC	Egg phosphatidylcholine
Chol	Cholesterol
ESM	Egg sphingomyelin
GMS	Glycerol monostearate
SA	Stearic acid
MCT	Medium chain triglycerides
GT	Glyceryltridecanoate
TG	Glyceryl tripalmitate
AEMA	2-aminoethyl methacrylamide
FA	Folic acid
TPGS	d-α-tocopheryl polyethylene glycol 1000 succinate
$E_{137}S_{18}E_{137}$	Block copolymer of ethylene oxide and styrene oxide
APTS	3-aminopropyl triethoxysilane
TEOS	Tetraethyl orthosilicate
βCD	β-cyclodextrin
HP-βCD	Hydroxypropyl-β-cyclodextrin
SBE-βCD	Sulfobutyl ether-β-cyclodextrin
SBE-7βCD	Sulfobutyl ether-7β-cyclodextrin
MLV	Multi-lamellar vesicles
aMPEG	Acrylated methoxy poly(ethylene glycol)

Boc-AEMA	Hydrophilic part and N-2-[(*tert*-butoxycarbonyl)amino] ethyl methacrylamide
mPLGA	Methacrylated poly(lactic-co-glycolic acid)
SPION	Superparamagnetic iron oxide
NLC	Nanostructured lipid carriers
LNCaP	Lymph Node Carcinoma of the Prostate
hCMEC	Human cerebral microvascular endothelial cells
iNOS	Inducible nitric oxide synthase
F_3O_4	Magnetite

- This page was intentionally left in blank –

CHAPTER 1. INTRODUCTION

1.1. QUERCETIN

1.1.1 HISTORY OF QUERCETIN

Quercetin (3,3´,4´,5,7-pentahydroxyflavone) is a flavonol isolated and identified for the first time by Szent-Gyorgyi in 1936 (Figure 1) [1]. In the beginning, and similarly to what happened with other flavonoids, quercetin was identified as a vitamin showing to be important in the maintenance of capillary wall integrity and capillary resistance antihypertensive and antiarrhythmic activity. In posterior studies it was proven to have anti-inflammatory and antiallergic properties, hypocholesterolaemic activity, platelet and mast cell stabilization, antihepatotoxic activity and antitumor activity [2, 3]. Later on, more profound works explained the reasons for this beneficial effects of quercetin based on antioxidant (free-radical scavenging) and anti-inflammatory activity [4].

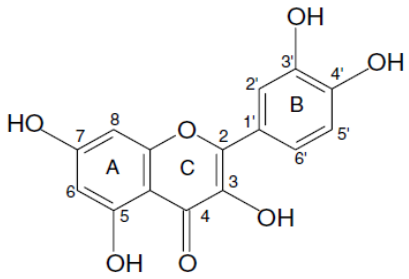

Figure 1. Chemical structure of quercetin.

1.1.2. NATURAL SOURCES OF QUERCETIN

Quercetin is one of the most abundant flavonoids in vegetables and fruits, mainly in onions, chilli, berries and apples (Table 1) [5-7]. It is present mainly in leaves as aglycones or glycosides (3-position or/and 4´-position). The most common sugar group found is glucose, however lactose and rhamnose can also be bound to phenolic groups of quercetin [5]. It is important to refer that in onion quercetin appears in the form of quercetin-4´-O-β-glucoside and quercetin-3,4´-O-β-diglucoside, representing 80% of the total content of quercetin flavonoid types, being present in high quantities in 28 vegetables and 9 fruits studied [8]. In a different study, quercetin was found in all 25 eatable berries studied and the highest concentration was found

in bog whortleberry (158 mg/kg, fresh weight) [9]. In a different work, quercetin-3-O-β-glucoside was found in a considerable amount in apple, pear peels, *Hypericum perforatum* leaves or flowers [5, 10]. Moreover, other studies have shown that black tea, red wine and various fruit juices can be valid choices as sources for quercetin [11].

Table 1. Quercetin natural sources [5, 9, 11].

Sources	Total quercetin (mg/Kg)
White onion bulbs	2604
Onion dry outer skin	960
Spring onion leaves	450
Chilli powder	400
Bog whortleberry	158
Lingonberry	146
Cranberry	121
Kale	110
Chokeberry	89
Sweet rowan	85
Rowanberry	63
Sea buckthorn berry	62
Apples red delicious	58
Crowberry	56
Broccoli	30
Green beans	25
Apple peel	21
Tomato	13

1.1.3 BIOSYNTHESIS OF QUERCETIN

The biosynthesis of quercetin shares almost the same steps in terms of metabolic pathway of the other flavonoids. The three-ring structure (A, B and C) with a diphenyl propane skeleton (C-6-C-3-C-6) is a fingerprint of quercetin (Figure 1) [3]. The A and B are benzene rings linked by oxygen containing pyrene ring (C) [12]. The A ring is biosynthesized by the condensation of three moles of malonyl-coenzyme A (CoA) originated from the metabolism of glucose [3]. The C and B rings are also derived from glucose metabolism by way of the shikimic acid pathway to produce cinnamic acid and its reduced product, coumaric acid [3]. As CoA derivatives, this C-9 *p*-coumaroyl-CoA

condenses with three moles of C-3 malonyl-CoA to form a C-15 chalcone. After that, the ring closes and the hydration gives rise to quercetin (Figure 2) [13].

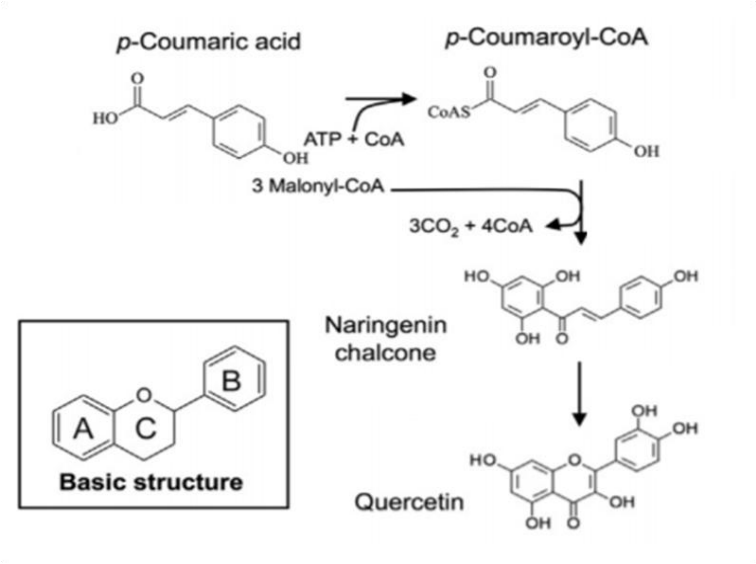

Figure 2. Schematic representation of quercetin biosynthesis.

1.1.4. CHEMICAL STRUCTURE AND PROPERTIES OF QUERCETIN

The IUPAC name of quercetin is 2-(3,4-dihydroxyphenyl)-3,5,7-trihydroxy-4H-chromen-4-one. This is composed by two benzene rings and one oxygen containing pyrene ring (Figure 1) [3]. Quercetin has amphipathic behavior due to the phenyl rings (hydrophobic part) and the hydroxyl groups (hydrophilic part) [14, 15]. Nevertheless, quercetin presents low water solubility. There is some controversy in the literature concerning its solubility value, however most studies indicate approximately 0.01 mg/mL (25°C) [16-18]. Besides that, photodegradation of quercetin is also an important issue to concern while working with this flavonoid. A photostability study has been conducted with quercetin alcoholic solutions and the results revealed the appearance of some products of degradation measured by spectrophotometry under the exposition to UVB and UVA radiation, indicating the degradation of this polyphenol compound [19]. Another important property relates with quercetin stability at different pH values. One study has demonstrated that quercetin is degraded at weak basic pH 8, while at pH 5 almost 75% of quercetin remains in solution, indicating that quercetin is more stable in a protic medium [20]. Furthermore, a magnetic study of quercetin indicates this compound displays diamagnetic properties [14]. This feature shows that valence electrons are paired and consequently the compound seems to be stable. However the

study of LUMO (lowest unoccupied molecular orbital) and HOMO (highest unoccupied molecular orbital) showed a little energy gap between those orbitals indicating that an electron can transit from LUMO to HOMO orbitals and by this way can easily react [14]. Additionally, the ionization potential study showed that it is easy to take away an electron from the valence orbital [14]. These two properties may explain the antioxidant capacity of quercetin.

1.1.5. ABSORPTION, DISTRIBUTION, METABOLISM AND ELIMINATION

Quercetin is a highly hydrophobic compound, so when it arrives to the small intestine, it can be absorbed by the epithelial cells passing through cellular membranes (phospholipid bilayers) by simple diffusion pathway [21]. Chen et al. performed some absorption experiments in Sprague–Dawley rats and found that almost 60% of quercetin orally administered was absorbed [22]. This result was comparable to the work developed by Walle et al. where 53% of quercetin administered was absorbed [23]. Inside the epithelial cells (enterocytes), the compound then suffers glucuronidation and sulfatation at one of the hydroxyl groups by glucuronosyltransferases and sulfotransferases (phase II enzymes) in order to confer hydrophilicity [24-27]. Quercetin can also be O-methylated, primarily resulting in the formation of 3´-O-methylquercetin (isorhamnetin) and, to a smaller extent, 4´-O-methylquercetin (tamaraxetin) [26, 27]. When quercetin is conjugated with sugars, the first step is to remove this group by β-glucosidase present in enterocytes and intestinal flora and after that the quercetin can be conjugated as previously mentioned [24]. However, some molecules of quercetin can enter the circulation without suffering any conjugation. These molecules will reach the liver through the portal vein and there will occur metabolization by glucuronosyltransferases and sulfotransferases, which are enzymes largely expressed [28]. Moreover the catechol-O-methyltransferase (COMT) enzymes present in liver and kidney can methylate quercetin [27, 29, 30]. If quercetin conjugates are excreted for bile they flow in the small intestine and they reach the hindgut where they can be hydrolyzed by the β-glucuronidase and sulfatase activities of the microflora, which allows the enterohepatic cycling, increasing the circulation time [28]. Although liver is the central organ of metabolization, a study shows that 90% of quercetin absorbed was metabolized in the gut [22]. All these enzymatic changes transform quercetin in a compound more soluble and allow blood circulation freely or bound to blood proteins, such as albumin [31, 32]. The entrance of quercetin in blood circulation will allow tissue distribution. It is also important to refer that quercetin can be absorbed from the gastrointestinal tract to the lymphatic system [26]. The regular ingestion of the

compound appears to accumulate in many organs (i.e., lung, kidney, thymus, heart, liver) with the highest concentrations of quercetin and its methylated derivatives, particularly isorhamnetin, found in the pulmonary tissue [33]. Quercetin remains in the organism for a long period of time (20-72 h) and probably this may be due to enterohepatic recycling [23]. However, quercetin can be degraded by microflora in the colon in phenolic acids and carbon dioxide, which is expelled in breath [34]. Consequently, the phenolic acids can be excreted in feces. Some quercetin may be also eliminated in urine [35-37]. All this routes are valid for quercetin elimination. In a study conducted by Ueno et al., quercetin was excreted as expired CO_2 (35%), or via the feces (45%) and urine (10%) as glucuronide or sulfate conjugates following oral administration [38]. However, in a more recent study only a small amount of absorbed quercetin was eliminated in urine (3.3–5.7%) and feces (0.21–4.6%) [23]. The majority of quercetin was eliminated under the form of carbon dioxide (41.8–63.9%) [23].

1.1.6. TOXICITY OF QUERCETIN

In terms of toxicity, there are still some contradictory results. The *in vitro* studies revealed that quercetin induces SOS activity, reverse mutations and DNA single strand breaks in bacteria (*Salmonella typhimurium* strains and *Escherichia coli*) and in eukaryotic cells, including yeast cells, at relatively high concentrations (up to 10 mg/incubation mixture) in the last case [39-42]. In hamster and mouse cells and human lymphocytes were verified special effects as chromosomal aberrations, DNA single strand breaks and micronucleus formation [43, 44]. However, this toxicity was not proven to occur in *in vivo* studies. Mice and rats oral administered with quercetin consistently did not induce any significant changes in several mutagenicity/genotoxicity endpoints, i.e., micronuclei, chromosomal aberrations, sister chromatid exchange, unscheduled DNA synthesis, and alkali-labile DNA damage [44-46]. Based on the toxicity founded by *in vitro* assays, the carcinogenity of quercetin was questioned using animal models. F344 rats receiving quercetin as 0.1% of the diet (50 mg/kg body weight/day) for a period of 540 days, did not differ from the control rats in terms of tumor incidence, with the exception of lung adenoma and one jejunal adenocarcinoma [47]. In order to comprove the connection between quercetin and lung cancer, quercetin was administered in the diet of A/JJms mice at 5% (7500 mg/kg body weight/day) for a period of 23 weeks, and this compound did not induce a significant difference in the incidence of lung tumors, discarding the possibility of quercetin to induce lung cancer [48]. Therefore, all studies conducted *in vivo* with animal models seem to indicate that quercetin is a safe compound.

1.1.7. HEALTH BENEFITS OF QUERCETIN

1.1.7.1. CANCER CHEMOPREVENTION

Quercetin has been reported as a cancer chemopreventive compound. This feature is associated to its ability to inhibit carcinogenesis via antimutagenic activity, antioxidant activity, anti-inflammatory mechanisms, modulation of signal transduction pathways, and apoptosis-inducing and anti-proliferative activity [49]. Aryl hydrocarbon receptor (AhR) which binds to polycyclic aromatic hydrocarbons (PAHs) and halogenated aromatic hydrocarbons (HAHs) can activate the expression of CYP1A1, CYP1A2, and CYP1B1 and consequently these enzymes have the capacity of activating procarcinogens resulting in lung cancer [50]. Quercetin seems to naturally bind to AhR, being capable of preventing this signalization cascade and consequently cancer [50, 51]. Quercetin have also the capacity of inducing the expression of death receptor 5 (DR5) in lung cancer cells which binds to TNF-related apoptosis-inducing ligand (TRAIL) and promotes apoptosis [52]. Additionally, quercetin can interfere with ErbB signalization pathway reducing the expression of ErbB2 and ErbB3 in HT-29 colon cancer cells resulting in the inhibition of cell growth and the induction of apoptosis [53]. Another important example relates with prostate cancer prevention. Quercetin demonstrates capacity to reduce the expression of androgen receptor (AR) in human prostate cancer cell lines, LNCaP and/or LAPC-4 slowing down the progression of cancer [54]. All these studies clearly show the capacity of quercetin to prevent and slowdown cancer and impair its progression.

1.1.7.2. CARDIOVASCULAR PROTECTION

Quercetin can protect the cardiovascular system by multiple pathways. Galindo et al. conducted a study with rats and showed that regularly intake of quercetin reduces the systolic blood pressure, normalizes the heart rate, reduces heart hypertrophy and allows aortic relaxation by increasing nitric oxide and reducing some subunits expression of NADPH oxidase [55, 56]. Furthermore, quercetin has the ability to activate fibrinolytic proteins (t-PA, u-PA, PAI-1, u-PAR and Annexin-II) in mice, which disrupt fibrin clots in blood vessels contributing to eliminate the thrombi and consequently lowering the risk of coronary heart diseases (CHD) [57]. Despite several studies showed the decrease of blood pressure in rats, it is necessary to transfer these studies into humans. Therefore, Edwards et al. proved that quercetin can lower the blood pressure in stage 1 hypertensive patients [58].

1.1.7.3. ANTI-INFLAMMATORY ACTION

Nowadays, many studies illustrate the anti-inflammatory capacity of this polyphenol compound. Mamani-Matsuda and colleagues have worked with rat models of arthritis, which correlates well to what happens in humans in terms of macrophage markers, and demonstrated that quercetin reduced the production of nitric oxide (NO), tumor necrosis factor (TNF-α), monocyte chemoattractant protein 1 (MCP-1) and interleukin 1 beta (IL-1β) which are the major inflammatory and pro-arthritic mediators of macrophages [59]. Additionally, Rogerio et al. used murine models of asthma to prove the capacity of quercetin to lower the number of white blood cells and eosinophil in the bronchoalveolar lavage fluid, blood and lung parenchyma [60]. Besides these studies in animal models, the anti-inflammatory ability of quercetin was also tested in human cells. Human mast cell lines were stimulated with phorbol 12-myristate 13-acetate (PMA) and calcium ionophore. Quercetin decreased the gene expression and production of TNF-α, interleukin-1β, IL-6, and IL-8 by reducing the activation of NF-kB and p38 mitogen-activated protein kinase [61]. Also with human mast cells, Kimata et al. demonstrated the capacity of quercetin to impair the release of histamine, leukotrienes, prostaglandin D2, and granulocyte macrophage-colony stimulating factor [62]. All these studies are strong evidences of the anti-inflammatory capacity of quercetin.

1.1.7.4. ANTIOXIDANT ACTIVITY

It is well known the antioxidant activity of quercetin. This natural compound participates in many protective mechanisms, such as, scavenging reactive oxygen species (ROS) and preventing ROS formation by chelating transition metal ions, such as, iron and copper [63, 64]. The radical scavenging ability of this flavonol is due to its chemical structure, particularly the hydroxyl (-OH) substitutions and the catechol-type B-ring [65]. There is many studies proving this capacity, namely the works developed by Kim and Jang who showed that quercetin had the ability to protect against the oxidative stress provoked by hydrogen peroxide in HepG2 cell line [66]. Moreover, Sánchez et al. proved that quercetin downregulates NADPH oxidase, increases endothelial nitric oxide synthase (eNOS) activity and prevents endothelial dysfunction in spontaneously hypertensive rats, highlighting also its cardiovascular protection through the oxidative stress reduction [56]. Besides that, Chen et al. demonstrated the inhibition of iNOS gene expression by quercetin in mouse BV-2 microglia [67].

1.1.7.5. NEUROPROTECTION EFFECTS

Several studies bring strong and solid evidences of quercetin neuroprotection activity. In fact, it can protect nerve cells from oxidative stress increasing the survival of neurons [68-70]. Simultaneously, it can induce neuron differentiation contributing to maintain the balance of neuron number [71]. Not only in preventing but also in the treatment of neurodegenerative disease, quercetin can be an interesting natural compound to attenuate the progressive degradation and loss of cell neurons. In this context, the accumulation of aggregates can cause a massive oxidative stress and, here, quercetin may play an important role. For example, in the case of Alzheimer's disease, Ansari et al. showed that quercetin was capable of reducing protein oxidation, lipid peroxidation and apoptosis caused by amyloid beta-protein, Aβ(1-42), in primary hippocampal cultures [72]. Moreover, this flavonol has also shown ability to inhibit the fibril formation of Aβ in a study conducted by Kim et al. [73]. Besides that, quercetin shows a varied spectrum of action in brain protection, such as increased mitochondrial biogenesis [74]. In fact, this is very important because impaired mitochondrial activity seems to be correlated with neurodegenerative diseases [49]. At same time, this natural compound is a potent anti-inflammatory and can reduce the expression of proinflammatory molecules contributing to reduce the damage associated to this destructive inflammation process [75].

1.2. NANOTECHNOLOGY

1.2.1 NANOPARTICLES TO DELIVER QUERCETIN

Nowadays, the challenge consists in trying to deliver drugs to their target places, allowing to increase compounds bioavailability, thereby lowering the amount of administered substances and, consequently, minimizing their side-effects while enhancing their therapeutic efficacy. This question is particularly important while dealing with hydrophobic molecules, being crucial to find the best vehicles to increase the solubility and bioavailability of these compounds, in order to reach their target areas. Quercetin is one of these examples and several studies reported on the literature devote great attention to the development of several nanotechnological approaches which try to establish the best strategy to encapsulate and deliver quercetin for different applications. Table 2 summarizes some parameters that characterize different quercetin delivery systems, namely their composition, particle size, zeta potential, entrapment efficiency, administration route and *in vitro*/*in vivo* results.

Table 2. Properties of different quercetin-loaded carriers.

NPs Type	Composition	Morphology	Particle size (nm)	Zeta potential (mV)	EE (%)	Administration route	*In vitro*/*in vivo* results	Refs
Liposomes	PC/Chol; EPC/Chol/PEG; lecithin/Chol/PEG; ESM/Chol/PEG	spherical	150 to 450	-20 to -30	65 to 95	oral, intranasal, intravenous, topical	- anxiolytic and cognitive-enhancing effects in rats; - hepatoprotective effects in rodents; - attenuation of edema and inflammation in irradiated mice; - inhibition of tumor angiogenesis, inhibition of tumor cell growth and induction of tumor cell apoptosis (cell lines and mice).	**[76-81]**
Lipid nanoparticles	GMS/soya lecithin/PEG; GMS/SA/MCT/soya lecithin; Compritol; GT/TG/soya lecithin	spherical	35 to 350	-10 to -35	85 to 95	oral, intravenous, topical	- enhancement of the oral absorption in rats; - increase of drug penetration in skin and anti-oxidation and anti-inflammation effect; - improvement of memory retention in rats with aluminum-induced dementia; - induction of tumor cell apoptosis in breast cancer cell lines.	**[82-86]**
Polymeric nanoparticles	PLA; PLGA; PLGA/PEG/AEMA; PLGA/PEG/FA; PCL/TPGS; PLGA/TPGS	spherical, bean-like shape	30 to 150	-5 to -40	60 to 98	intravenous, topical	- enhancement of cancer cell uptake in tumor-bearing mice; - increase of cytotoxicity and induction of apoptosis in breast and liver hepatocellular carcinoma cell lines; - block/reduce of histological alterations in irradiated mice; - enhancement of neuron cells viability due to inhibition of aβ-42 peptide neurotoxicity in cell lines; - improvements of cognition and memory impairments in	**[87-94]**

							APP/PS1 mice model of Alzheimer's disease.	
Magnetic nanoparticles	Fe_3O_4; $Fe_3O_4/E_{137}S_{18}E_{137}$; Fe_3O_4/APTS/PEG/FA; Fe_3O_4/PLGA	spherical	10 to 300	around +6	around 80	Intranasal	- induction of cytotoxicity in human lung carcinoma, breast cancer and glioblastoma cell lines.	**[95-98]**
Mesoporous silica nanoparticles	TEOS/APTS; TEOS/FA	spherical	200 to 250	-25 to +13	around 99	n.i.	- inhibition of tumor cell proliferation and induction of tumor cell apoptosis (cell lines).	**[99, 100]**
Cyclodextrins	βCD; HP-βCD; SBE-βCD; SBE-7βCD	truncated cone; fibers	around 270	n.i.	n.i.	Oral	- increase of quercetin solubility and photostability; - enhancement of quercetin antioxidant capacity; - inhibition of tumor cell proliferation in cell lines; - impairment of tumor growth in B16F10 mouse melanoma model.	**[101-104]**

n.i. – not indicated; PC – phosphatidylcholine; EPC – egg phosphatidylcholine; Chol – cholesterol; PEG – poly(ethyleneglycol); ESM – egg sphingomyelin; GMS – glycerol monostearate; SA – stearic acid; MCT – medium chain triglycerides; GT – glyceryltridecanoate; TG – glyceryl tripalmitate; PLA – poly(lactic acid); PLGA – poly(lactic-co-glycolic) acid; PCL – poly(ε-caprolactone); AEMA – 2-aminoethyl methacrylamide; FA – folic acid; TPGS – d-α-tocopheryl polyethylene glycol 1000 succinate; $E_{137}S_{18}E_{137}$ – block copolymer of ethylene oxide and styrene oxide; APTS – 3-aminopropyl triethoxysilane; TEOS – tetraethyl orthosilicate; βCD – β-cyclodextrin; HP-βCD – hydroxypropyl-β-cyclodextrin; SBE-βCD – sulfobutyl ether-β-cyclodextrin; SBE-7βCD – sulfobutyl ether-7β-cyclodextrin.

1.2.2. NANOTECHNOLOGY STRATEGIES FOR THE DELIVERY OF QUERCETIN

1.2.2.1. LIPOSOMES

Liposomes can be developed as nanocarriers which mimetize the cellular phospholipid bilayers. The phospholipids used to produce liposomes have hydrophilic and hydrophobic portions allowing the spontaneous formation of spherical lipid bilayers in water formulations. The type of lipids chosen influences the properties of liposomes, such as charge, size, rigidity, etc. [105]. Liposomes composed by natural phospholipids are biologically inert and weakly immunogenic which is crucial to biological applications [106]. Liposomes have been used to encapsulate quercetin for many purposes [76-81, 107]. Liu et al. have developed liposomes composed by phosphatidylcholine, cholesterol and tween 80 to encapsulate quercetin in order to protect the hairless skin of Kun Ming mice against photodamage provoked by UVB [79]. Shaji et al. used multi-lamellar vesicles (MLV) with phosphatidylcholine and cholesterol in ratio of 9:1 to encapsulate quercetin and showed hepatoprotective activity in rats [77]. Thinking in tumoral therapy, Yuan et al. made a work with tumor-bearing mice model using lecithin/cholesterol/PEG4000/quercetin in 13:4:1:6 ratio and showed tumors growth inhibition [78]. Particularly, Long et al. used PEGylated liposomes composed by lecithin and cholesterol to encapsulate quercetin showing anti-tumor and anti-angiogenesis properties in ovarian cancer mouse model [79]. Many times, it is advantageous to use the synergistic effect of drugs to treat cancer. With this in mind, Wong et al. used liposomes to encapsulate vincristine and quercetin for treatment trastuzumab-insensitive breast tumor xenograft model [80]. This formulation was capable of increasing the circulation time of both drugs in plasma and inhibiting tumor growth [80]. For brain application area, Priprem et al. used quercetin liposomes in rats, with a mixture of egg phosphatidylcholine, cholesterol, and quercetin (2:1:1) and dispersed in 50% polyethylene glycol in water and they managed to reduce the anxiety and verified cognitive-enhancing in rats [76], while Phachonpai et al. have also developed egg phosphatidylcholine/cholesterol liposomes to encapsulate quercetin and showed promising results via intracerebroventricular route administration, reducing degeneration of cholinergic neurons in hippocampus [107]. Finally, in human cell lines, Goniotaki et al. demonstrated that quercetin encapsulated in egg phosphatidylcholine liposomes can inhibit the growth of many human cancer cells [81].

1.2.2.2. LIPID NANOPARTICLES

Lipid nanoparticles can be classified as nanostructured lipid carriers (NLC) and solid lipid nanoparticles (SLN) [108]. The last one is composed by one or more solid lipids which form a solid matrix, being excellent vehicles for drug delivery because of its physical stability, protection of the incorporated drug from degradation, controlled release and low cytotoxicity [109]. Despite these advantages, their lipid matrix may suffer recrystallization while stored and form more perfect matrices (β-modifications) that can prematurely release the encapsulated compound [110]. In this context, NLC have been developed to overcome this problem, because they blend liquid lipids with solid ones, creating an imperfect structure with more cavities and capacity to encapsulate drugs and avoiding premature release of the encapsulated compounds [110]. Several approaches using lipid nanoparticles have been developed in order to increase quercetin bioavailability and target specific places [82-86]. Li et al. produced SLN with glyceryl monostearate and soya lecithin, registering increased quercetin gastrointestinal absorption in rats [82]. However, it is also possible to think in topical administration of quercetin in order to protect against oxidative stress in skin caused by multiple factors (radiation, stress, etc.). Bose et al. have performed some permeations studies using Franz diffusion cells with human skin and SLN composed by precirol and compritol in 3:2 ratio were capable of increasing the content of quercetin inside skin demonstrating the lipid nanoparticles have great capacities as nanocarrier for topical delivery [84]. This idea was confirmed by Chen-yu et al. using glyceryl monostearate, stearic acid and media chain triglyceride to prepare NLC for topical administration in ear edema induced rats. The results showed a suppression of edema in the animals [83]. This capacity to protect against oxidative stress can be used in cancer therapy because many times cancer formation and progress are associated with multiple mutations that can be caused by ROS. In a study conducted by Sun et al. it was possible to induce apoptosis of MCF-7 and MDA-MB-231 breast cancer cells using NLC composed by 2.7% quercetin, 9.4% soy lecithin, 23.6% glyceryltridecanoate, 6.7% glyceryl tripalmitate, 13.4% vitamin E acetate and 44.2% Kolliphor HS15 [85]. Besides that, taking advantage of its neuroprotection properties, Dhawan et al. encapsulated quercetin in SLN composed by compritol and tween 80 [86]. They tested this formulation in rats chronically administered with aluminum chloride which causes an oxidative stress responsible for brain damaged [86]. The results showed that quercetin loaded SLN were capable of improving memory retention in rats with aluminum-induced dementia comparing to quercetin alone and empty nanoparticles, indicating that this nanosystem may be efficient to target brain [86].

1.2.2.3. POLYMERIC NANOPARTICLES

Polymeric nanoparticles are made of biodegradable polymers that may offer multiple advantages, like being stable in blood, non-toxic, nonthrombogenic, nonimmunogenic, noninflammatory, do not activate neutrophils, biodegradable, avoid reticuloendothelial system and applicable to various molecules such as drugs, proteins, peptides, or nucleic acids [111]. The versatility of these nanoparticles is based in the capacity of choosing the best polymer to the desired application. By this way these nanomedicines have been used in many approaches [87-94]. Kumari et al. synthesized polylactic acid (PLA) nanoparticles with high encapsulation efficiency and controlled release of quercetin making them promising for therapy [87]. Khoee et al. used methacrylated poly(lactic-co-glycolic acid) (mPLGA) as a lipophilic domain, acrylated methoxy poly(ethylene glycol) (aMPEG) as hydrophilic part and N-2-[(*tert*-butoxycarbonyl)amino] ethyl methacrylamide (Boc-AEMA) as pH-responsive part. They have proven the capacity of these polymeric nanoparticles to release their content in acidic environment and showed that they are suitable for cancer therapy [88]. El-Gogary et al. produced PEGylated PLGA nanoparticles conjugated with folic acid and demonstrated the capacity of these quercetin loaded nanosystems of increasing the killing capacity in HeLa cells compared to quercetin alone [89]. At the same time, the tumor uptake was confirmed in injected tumor-bearing mice [89]. Finally, Bishayee et al. used gold-quercetin into PLGA nanoparticles as special system to escape the immune attack [90]. The results showed that these nanoparticles had the ability to control proliferation and induce apoptosis in hepatocarcinoma cells [90].

1.2.2.4. MAGNETIC NANOPARTICLES

Magnetic nanoparticles are very promising nanosystems whose magnetic properties allow to control and direct them to the target place applying an exterior magnetic field [112]. It is also interesting to notice that, below a certain range of size (10-20 nm), magnetic nanoparticles behave like a giant paramagnetic atom with a fast response to applied magnetic fields with negligible remanence (residual magnetism) and coercivity (the field required to bring the magnetization to zero) [113]. The absence of residual magnetism is crucial because agglomeration can be prevented [113]. So far, there are not so many applications using magnetic nanoparticles to encapsulate quercetin, however their use now starts to take its first steps [95-98]. For instance, magnetic nanoparticles are very promising for cancer therapy because external magnetic fields can direct them to the cancer area. Taking this in consideration and thinking on the

cancer chemotherapeutic properties of quercetin, magnetic nanoparticles have to be considered as potential and promising nanosystems for delivering quercetin in tumor cells. In a preliminary study, Barreto et al. synthesized Fe_3O_4 nanoparticles and showed that these magnetic nanoparticles had a controlled releasing time making this vehicle promising for cancer chemotherapy [95]. This study was followed by some studies of concrete applications of magnetic nanoparticles to deliver quercetin. Verma et al. used Fe_3O_4 magnetic core-shell nanoparticles protected against oxidation by PLGA and tested this formulation in the human lung carcinoma cell line A549 [96]. The results showed that quercetin loaded PLGA-MNPs had no toxicity after injection in mice and at the same time they were able to reduce the number of A549 viable cells demonstrating an anti-cancer capacity [96]. In other study conducted by Kumar et al. quercetin superparamagnetic Fe_3O_4 nanoparticles were tested *in vitro* to analyze the effects in breast cancer cell lines [97]. Fluorescent microscopy demonstrated changes in cellular morphology of MCF7 cells treated with these quercetin loaded nanoparticles indicating cytotoxicity for cancer cells and consequently potential for cancer therapy [97]. Additionally, for target brain cancer Akal et al. designed superparamagnetic iron oxide (SPION), which was functionalized with APTES ((3-aminopropyl) triethoxysilane), polyethylene glycol (PEG) and folic acid [98]. Folic acid was strategically used in order to target brain adenocarcinoma cells (U87) which overexpress folic acid receptors [98]. The MTT analysis after cellular uptake of SPION loaded with quercetin demonstrated decreasing of cancer cell viability [98]. Together, these results showed clear evidence that magnetic nanoparticles are excellent vehicles to deliver quercetin and can be used for cancer therapy based on the mentioned studies.

1.2.2.5. MESOPOROUS SILICA NANOPARTICLES

Mesoporous silica nanoparticles (MSN) are becoming very attractive since they are biocompatible, stable, have a tunable size pore, high drug encapsulation, slow drug release and possibility of functionalizing the surface [114-118]. Some studies concern the use of MSN as vehicles for quercetin delivery [99, 100]. Sapino et al. used MSN functionalized with aminopropyl for topical delivery of quercetin [99]. The results have shown that MSN increase the penetration of quercetin in the skin and, at the same time, inhibit the proliferation of R8 human melanoma cells [99]. In another work, MSN functionalized with folate, for targeting breast cancer cells, managed to cell cycle arrest and apoptosis in breast cancer cells through the regulation of Akt & Bax signalling pathways [100].

1.2.2.6. CYCLODEXTRINS

Cyclodextrins (CDs) are nanosystems similar to a truncated cone with a hydrophobic cavity and a hydrophilic surface. In the cavity it is possible to accommodate lipophilic drugs and deliver them to their target place [119]. Chemically, CDs are cyclic oligosaccharides with six, seven or eight glucose residues linked by glycosidic bonds [120]. There are a few applications of CDs as nanodelivey systems to encapsulate quercetin [101-104]. The inclusion of the quercetin inside β-cyclodextrin (β-CD), hydroxypropyl-β-cyclodextrin (HP-β-CD) and sulfobutyl ether-β-cyclodextrin (SBE-β-CD) has been studied [101, 102]. The results demonstrate that (SBE-β-CD) can encapsulate more quercetin than the other ones and, at the same time, may increase its antioxidant properties [101, 102]. Moreover, Aytac et al. used quercetin/β-cyclodextrin inclusion complex demonstrating the slow release of quercetin [103]. All these promising features as nanocarriers for quercetin were confirmed in a study conducted by Kale et al. [104]. They used ether-7β-cyclodextrin/quercetin complex in melanoma mouse models and verify the decrease of microvessels and consequently the reduction of tumor cell proliferation [104].

1.3. DISSERTATION WORK PLAN

1.3.1. PROBLEM AND MOTIVATION

Neurodegenerative diseases represent a major and growing public health burden. Currently, there are no treatments available and medications only treat symptoms, but do not halt or retard neurodegeneration process. Quercetin, a flavonol found in many plants and fruits, may provide protection against neurological disorders, such as Alzheimer's disease [121]. However, this polyphenol presents low water-solubility, chemical instability, rapid degradation and extensive metabolism, resulting in poor bioavailability which, therefore, compromises its arrival and delivery into the brain [122].

1.3.2. OBJECTIVE AND STRATEGY

The goal of this dissertation will be the development of nanocarriers for enhancing the bioavailability of quercetin, promoting its site-specific delivery through the blood-brain barrier (BBB) into the brain with the utmost purpose of treating or preventing Alzheimer's disease (Figure 3). Given the lipophilic characteristics of quercetin, lipid-based nanoparticles will be employed providing physical stability and compatibility, conferring protection from degradation and controlling the transport and brain delivery.

Moreover, nanoparticles surface will be functionalized with two distinct ligands: transferrin (Tf) and a 29 aminoacid peptide derived from the rabies virus glycoprotein (RVG29). The transferrin receptor (TfR) is highly expressed on the luminal side of brain capillary endothelium and might lead to receptor-mediated transcytosis of Tf-coated nanoparticles across the BBB [123]; while RVG29 was proven capable of transporting cargoes into the brain in a selective fashion [124] and binds specifically to the nicotinic acetylcholine receptor (nAchR) on neuronal cells, enabling the delivery of quercetin on damaged brain cells [125].

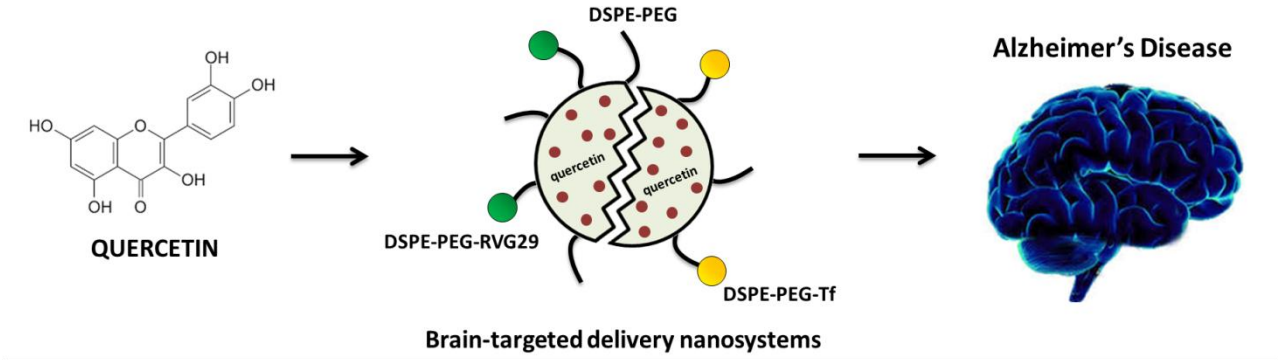

Figure 3. Schematic representation of the strategic plan

1.3.3. METHODS AND DETAILED DESCRIPTION

Task 1 - Preparation of lipid-based nanoparticles and functionalization with Tf and RVG29

Solid lipid nanoparticles (SLN) and nanostructured lipid carriers (NLC) were produced by a modified hot homogenization technique [126]. An average size around 200 nm was important to promote a longer circulation time and to enhance the permeability through the BBB [127]. Nanoparticles were loaded with quercetin and coated with polyethylene glycol (PEG) in order to reduce their hepatic clearance and prolong their blood circulation. Tf and RVG29 were covalently conjugated to the nanoparticles. The carboxyl groups of Tf were coupled to the amino groups of DSPE-PEG-NH_2 and the thiol groups of RVG29 specifically react with the maleimide groups of DSPE-PEG-MAL, previously conjugated to the nanoparticles surface.

Task 2 - Physicochemical characterization of the developed nanosystems

The developed nanosystems were fully characterized to evaluate the quality of the nanoparticles for brain delivery:

- Morphology was visualized by transmission electron microscopy (TEM);

- Hydrodynamic diameter, polydispersity index and zeta potential were measured by dynamic light scattering (DLS);
- Quercetin entrapment efficiency was determined by spectrophotometric analysis;
- The presence of Tf and RVG29 on the surface of nanoparticles were confirmed by Fourier transform infrared spectroscopy (FTIR) and nuclear magnetic resonance (NMR) spectroscopy.

Task 3 - *In vitro* validation of the developed nanosystems using cell lines and amyloid-beta peptide

The effectiveness of the nanodelivery systems for improving quercetin brain uptake was confirmed using hCMEC/D3 cell line as a model of the human BBB. Lactate dehydrogenase (LDH) assay was conducted to evaluate cell membrane integrity, after exposition to the nanoparticles. BBB permeability studies were performed using transwell culture systems. Finally, the aggregation process of the amyloid-beta peptide after nanoparticles incubation was assessed by ThT binding assay, since Aβ(1–42) is a promising target for the treatment of Alzheimer's disease.

1.3.4. TIMELINE

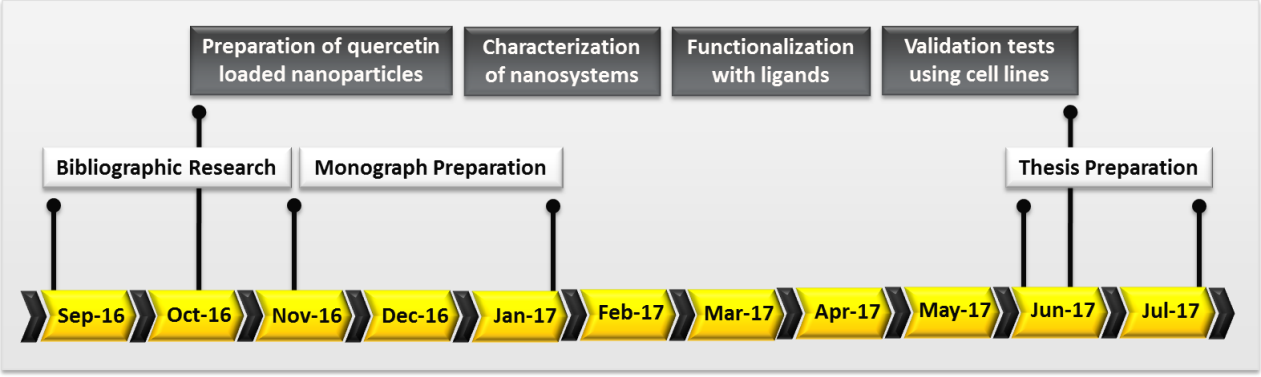

Figure 4. Tentative timeline (from September 2016 to July 2017).

CHAPTER 2. MATERIALS AND METHODS

2.1. PREPARATION OF NANOPARTICLES

Lipid nanoparticles were produced according to an optimized hot homogenization technique followed by sonication previously developed in our group [126, 128]. SLN were prepared using cetyl palmitate as the solid lipid, while NLC were produced using cetyl palmitate as the solid lipid and miglyol-812 as the liquid lipid. Polysorbate 80 was used as surfactant in the synthesis of both SLN and NLC (Table 3). The method applied consisted in warming up the lipid and aqueous phases separately at 80°C until the lipids were melted. The lipid phase was composed by lipids, surfactant and quercetin. The aqueous phase was then added to the molten lipid mixture. In order to control the size of particles, Ultra-Turrax T25 (Janke and Kunkel IKA-Labortechnik, Staufen, Germany) was used to form microparticles, followed by sonication in a Sonics and Materials Vibra-Cell™ CV18 (Newtown, CT, USA) to produce particles in the nanometer range. SLN were stirred for 30 seconds at 12000 rpm, followed by 5 minutes of 80% intensity sonication, while NLC were homogenized for 2 minutes and then sonicated during 15 minutes at 70% intensity.

Table 3. Composition of the synthetized lipid nanoparticles (SLN - solid lipid nanoparticles and NLC - nanostructured lipid carriers).

Formulation code	Cetyl palmitate (mg)	Miglyol-812 (mg)	Polysorbate 80 (mg)	Quercetin (mg)	Ultra-pure water (mL)
SLN Placebo	500	0	150	0	4.4
SLN Quercetin	500	0	150	10	4.4
NLC Placebo	350	150	150	0	4.4
NLC Quercetin	350	150	150	10	4.4

2.2. FUNCTIONALIZATION OF NANOPARTICLES WITH TRANSFERRIN

Nanoparticles were functionalized using 1,2-distearoyl-sn-glycero-3-phosphoethanolamine (DSPE) associated with polyethylene glycol (PEG) and terminal amine groups (NH_2) exposed on the nanoparticles surface. These last amine groups were conjugated with carboxyl groups of transferrin, thereby forming peptide bonds (Figure 5). Nanoparticles were prepared as previously described but incorporating 5 mg of DSPE-PEG-NH_2 in the lipid phase composition (Table 4). At the same time, a transferrin solution was prepared in ultra-pure water (5 mg/mL) and then the carboxyl groups of transferrin were activated with 1-Ethyl-3-(3-dimethylaminopropyl) carbodiimide (EDC) at room temperature, with stirring, for 30 minutes. After that, the transferrin solution was mixed with the previously produced nanoparticles conjugated with DSPE-PEG-NH_2 and the formulations were incubated for 2 hours, at room temperature. Finally, the Tf-functionalized nanoparticles were dialyzed in a 10 kDa MWCO SnakeSkin Dialysis Tubing against 500 mL ultra-pure water at 37°C, overnight, to remove the excess of transferrin and by-products.

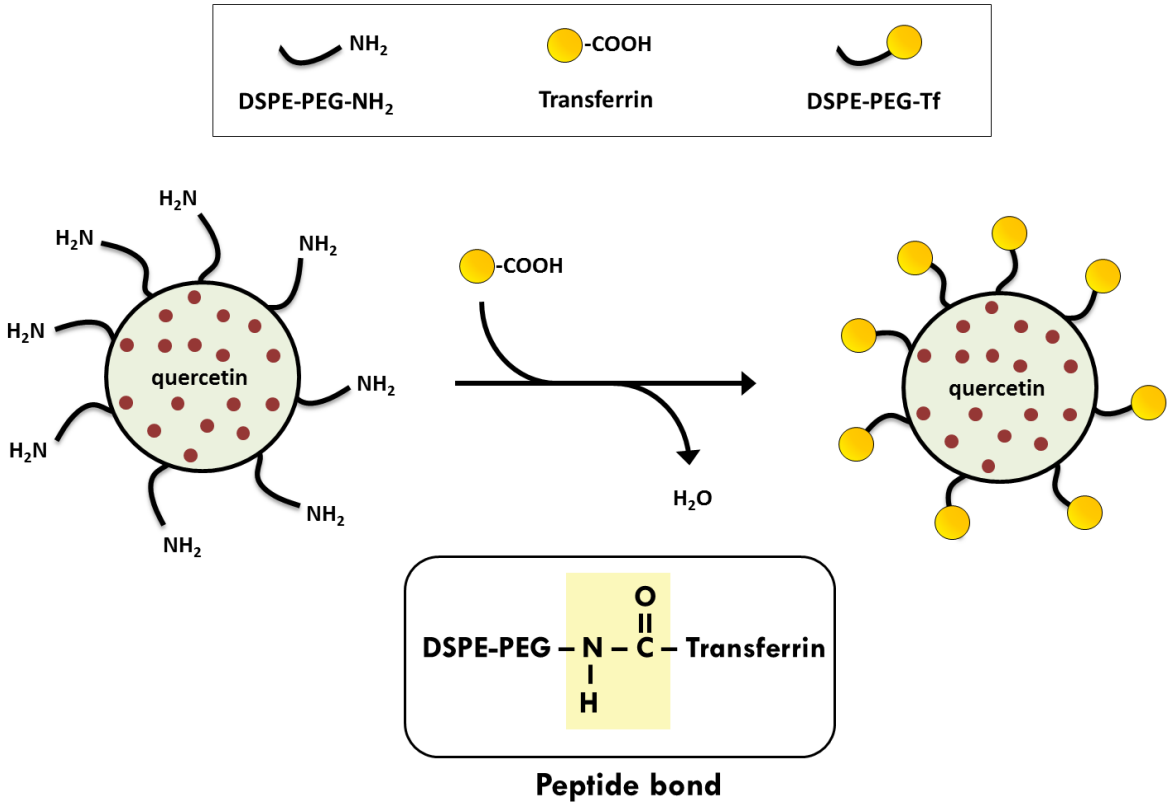

Figure 5. Schematic representation of the functionalization of nanoparticles with transferrin ligands (not to scale).

Table 4. Composition of Tf-functionalized lipid nanoparticles.

Formulation code	Cetyl palmitate (mg)	Miglyol-812 (mg)	Polysorbate 80 (mg)	DSPE-PEG-NH_2 (mg)	Transferrin (mg)	Quercetin (mg)	Ultra-pure water (mL)
SLN-Tf Placebo	500	0	150	5	5	0	4.4
SLN-Tf Quercetin	500	0	150	5	5	10	4.4
NLC-Tf Placebo	350	150	150	5	5	0	4.4
NLC-Tf Quercetin	350	150	150	5	5	10	4.4

2.3. FUNCTIONALIZATION OF NANOPARTICLES WITH RVG29

For surface modification of nanoparticles with RVG29 peptide, DSPE-PEG-MAL was previously conjugated to RVG29. DSPE-PEG-MAL is a 1,2-distearoyl-sn-glycero-3-phosphoethanolamine (DSPE) associated with polyethylene glycol (PEG) and terminal maleimide groups (MAL). The maleimide groups can react with thiol groups of RVG29, thereby forming thioether bonds (Figure 6). RVG29 peptide is a 29 amino acid fragment derived from rabies virus glycoprotein (RVG). The peptide RVG29 with an additional cysteine on C-terminal (YTIWMPENPRPGTPCDIFTNSRGKRASNGC) was synthesized by Bachem Group (Germany). Hence, a RVG29 solution (5mg/mL) was prepared in PBS (pH 7.0) followed by the addition of 1-fold DSPE-PEG-MAL. The mixture was allowed to react at room temperature for 24 hours, thus forming the conjugate DSPE-PEG-RVG29. The conjugate was then dialyzed in a 10 kDa MWCO SnakeSkin Dialysis Tubing against 500 mL ultra-pure water at 37°C, overnight, to remove the excess of RVG29 and by-products. Finally, nanoparticles were produced as previously described but incorporating 1 mL of DSPE-PEG-RVG29 conjugate in the lipid phase composition (Table 5).

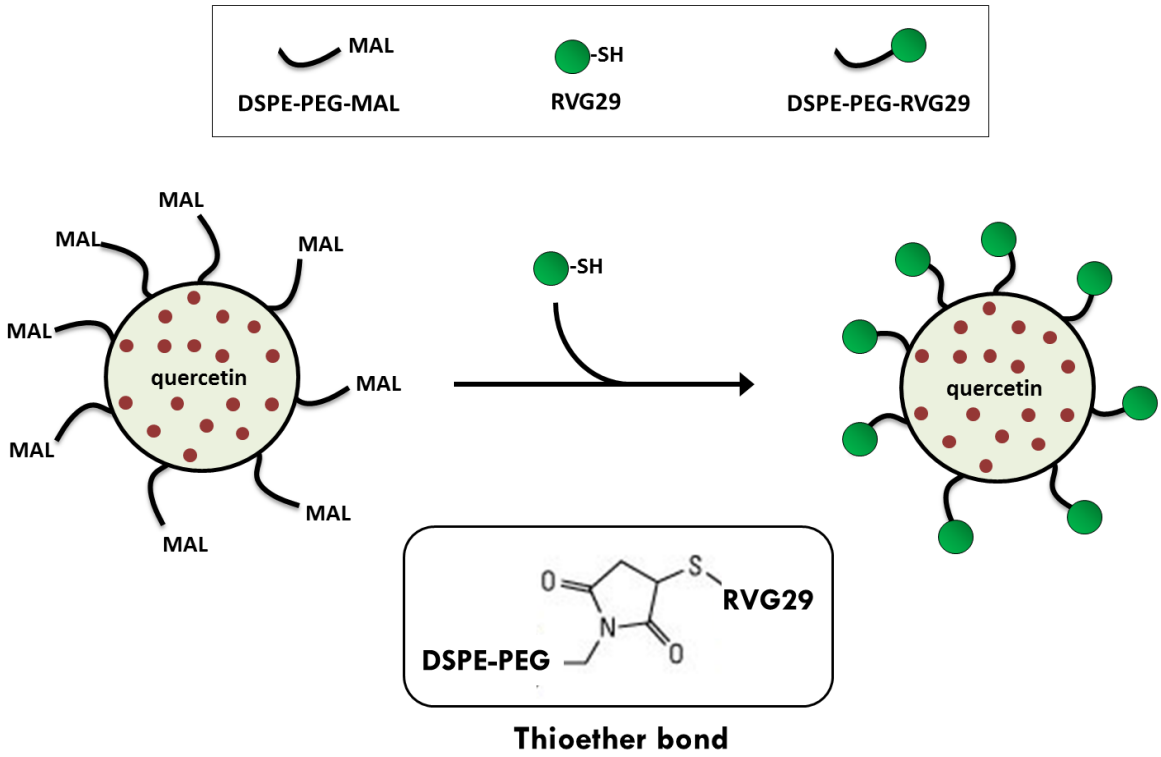

Figure 6. Schematic representation of the functionalization of nanoparticles with RVG29 ligands (not to scale).

Table 5. Composition of RVG29-functionalized lipid nanoparticles.

Formulation code	Cetyl palmitate (mg)	Miglyol-812 (mg)	Polysorbate 80 (mg)	DSPE-PEG-RVG29 (mL)	Quercetin (mg)	Ultra-pure water (mL)
SLN-RVG Placebo	500	0	150	1	0	4.4
SLN-RVG Quercetin	500	0	150	1	10	4.4
NLC-RVG Placebo	350	150	150	1	0	4.4
NLC-RVG Quercetin	350	150	150	1	10	4.4

2.4. NUCLEAR MAGNETIC RESONANCE SPECTROSCOPY

The successful synthesis of DSPE-PEG-Transferrin and DSPE-PEG-RVG29 conjugates were analyzed by NMR spectroscopy. NMR experiments were recorded on a Bruker Avance III 600 HD spectrometer (Bruker, Massachusetts, United States),

operating at 600.13 MHz for ^{1}H, equipped with 5 mm CryoProbe Prodigy and pulse gradient units, capable of producing magnetic field pulsed gradients in the z-direction of 50 G cm1. The NMR measurements were carried out in deuterium oxide (D_2O), at 300K and a spectral width of 10 000 Hz. ^{1}H NMR experiments were performed with water suppression using excitation sculpting with gradients. The chemical shifts of the ^{1}H NMR signals were referred to the absorption frequency of trimethylsilylpropanoic acid-d4 (TMSP-d4) as internal reference.

2.5. FOURIER TRANSFORM INFRARED SPECTROSCOPY

Fourier transform infrared spectroscopy (FT-IR) was used to confirm the functionalization of the nanoparticles with transferrin and RVG29 ligands. In order to perform this technique the samples were previously lyophilized in order to eliminate water bands that could mask the ones related to the sample itself. The first step of the lyophilization consisted in freezing the samples overnight in a -85°C deep freezer. After that, samples were lyophilized at -85°C and 0.76 Torr using a LyoQuest -85 freeze dryer (Telstar, Terrassa, Spain). Finally, the infrared spectra of the lyophilized nanoparticles were obtained using a Frontier FT-IR Spectrometer from PerkinElmer (Santa Clara, California, USA).

2.6. TRANSMISSION ELECTRON MICROSCOPY

The morphology of nanoparticles was analyzed by transmission electron microscopy (TEM). The samples were mounted on 300 mesh form var copper grids and were analyzed using a Jeol JEM 1400 transmission electron microscope (Tokyo). Uranyl acetate was used as the contrast agent. Images were digitally recorded using a Gatan SC 1000 ORIUS CCD camera (Warrendale, PA, USA).

2.7. DYNAMIC LIGHT SCATTERING

The mean hydrodynamic diameter of nanoparticles was measured by dynamic light scattering (DLS) using a particle size analyzer (Brookhaven Instruments, Holtsville, NY, USA). All samples were diluted in ultra-pure water by a factor of 1:400 before measuring the particles size. All determinations were made at 25°C with a light incidence angle of 90°. The hydrodynamic diameter followed a Gaussian distribution and polydispersity index was determined according to the width of particle size distribution.

2.8. ZETA POTENTIAL ANALYZER

The zeta potential of nanoparticles was calculated by measuring the electrophoretic mobility in a zeta potential analyzer (Brookhaven Instruments, Holtsville, NY, USA). All samples were diluted in ultra-pure water by a factor of 1:400 and all the measurements were performed at 25°C.

2.9. ENTRAPMENT EFFICIENCY DETERMINATION

All samples were diluted in ultra-pure water by a factor of 1:200 and filtered through 3.0 µm Millipore-type SSWP membrane filters. Nanoparticles can pass through the membrane filters, while unentrapped quercetin is retained on the filters. The quercetin retained in the filter was then recovered using 2 mL of acetonitrile on disposable syringes and the absorbance was measured in a V-660 spectrophotometer (Jasco, Easton, MD, USA) at 367 nm. Quercetin entrapment efficiency was obtained by the following equation:

$$EE\ (\%) = \frac{Total\ quercetin - Unentrapped\ quercetin}{Total\ quercetin} \times 100$$

2.10. PHOTOSTABILITY STUDY

Photostability studies were performed to investigate the protection effect of lipid nanoparticles against photodegradation of quercetin. Ethanol solutions of quercetin (0.7 mg/mL) and quercetin-loaded nanoparticle formulations were exposed to UVA light (HSW 125W E27, Sylvania) in a chamber with reflecting walls and a cooling system. The UV lamp had an emission spectrum between 320 and 400 nm, with an irradiation intensity of 5.5 x 10^{-3} kJ/s/m^2. After 6 h of UV light exposure, aliquots were withdrawn from each sample and diluted with acetonitrile by a factor of 1:200. In the case of nanoparticles, acetonitrile promote the disruption of lipid matrix, allowing the quantification of quercetin in solution by spectrophotometric detection at 367 nm in a V-660 spectrophotometer (Jasco, Easton, MD, USA). Quercetin photodegradation was calculated as a percentage by comparing the absorbance of quercetin at the endpoint to the maximum absorbance at the beginning of the experiment.

2.11. HCMEC/D3 CELL CULTURE

Immortalized human cerebral microvascular endothelial cells (hCMEC/D3) were obtained from Institut National de la Santé et de la Recherche Médicale (INSERM, Paris, France). This brain endothelial cell line is commonly used as a BBB model

system, since it mimics structurally and morphologically the human BBB properties [129, 130]. hCMEC/D3 cells were used between passage number 29 and 35. Cells were seeded in a concentration of 2.5 × 10^4 cells/cm^2 and grown at 37 °C, in an atmosphere of 5 % CO_2 in EndoGRO medium supplemented with 1% Pen-Strep, 5% FBS, 50 µg/mL ascorbic acid, 0.75 U/mL heparin sulfate, 1.0 µg/mL hydrocortisone hemisuccinate, 10 mM L-Glutamine and 5 ng/mL rhEGF. All culture flasks were pre-coated with 0.1 mg/mL type I rat collagen, 1 h at 37 °C. Cell culture medium was changed every 2–3 days.

2.12. LDH CYTOTOXICITY ASSAY

Lactate dehydrogenase (LDH) assays were conducted in order to evaluate cytotoxicity and nanoparticles potential for damaging cell membranes. LDH is an enzyme that is released from cells to the surrounding cell culture supernatant when cell membranes are damaged or disrupted. Cells were seeded in 96-well plates (10^4 cells per well) pre-coated with type I rat collagen. After 20 h of incubation at 37 °C and 5 % CO_2, different concentrations of quercetin-loaded nanoparticles (functionalized and non-functionalized) were incubated with the cells for 4 h. EndoGRO medium and TX-100 sample were also used as negative and positive controls for cytotoxicity, respectively. After the incubation time, the medium of each well was collected and centrifuged (250 g for 10 min, RT) and the supernatant separated for further LDH quantification assay (LDH cytotoxicity detection kit, Takara Bio Inc, Shiga, Japan). After treatment with catalyst and dye solutions for 20 min at RT in the dark, absorbance was read at 490 and 690 nm using a Synergy™ HT Multi-mode Microplate Reader (BioTek Instruments Inc, Winooski, VT, USA). Cytotoxicity was expressed as a percentage compared to the maximum cytotoxicity of TX-100 sample.

2.13. TRANSWELL PERMEABILITY ASSAY

hCMEC/D3 cells were seeded in a density of 2 x 10^5 cells per insert on transwell devices (six-well polyester inserts, pore size 0.4 µm and a diameter of 4.67 cm^2) precoated with type I rat collagen. The permeability assay was performed 7 days after seeding. The barrier integrity of hCMEC/D3 cell monolayers was previously checked using Lucifer Yellow as a small reference molecule with a well reported effective permeability coefficient (P_{eff}) of 1.33x10^{-3} cm/min [131]. For the permeability studies, functionalized and non-functionalized nanoparticles previously loaded with FITC (0.4 mg/mL) were incubated in the apical donor compartment for 4 h at 37°C in a 5% CO_2

atmosphere incubator. The total amount of nanoparticles in the receptor compartment was quantified after 0.5, 1, 2, 3 and 4 h by fluorescence analysis (495/519 nm).

2.14. AMYLOID-BETA PEPTIDE PREPARATION

Aβ(1–42) peptide (purity > 95%, MW 4514.14) was purchased from Selleck Chemicals. The aggregation state and the structure can vary according to the sample batch [132]. In order to solve the residual peptide aggregation and consequently improve its solubility, the peptide was previously dissolved in HFIP (1,1,1,3,3,3-hexafluoro-2-propanol) at 1 mg/mL in order to disrupt intermolecular H-bonds [133-135]. This solution was then evaporated with nitrogen flow and under vacuum and the resulting peptide film was dissolved in dimethyl sulfoxide at 9 mg/mL.

2.15. THIOFLAVIN T BINDING ASSAY AND FLUORESCENCE MEASUREMENTS

Thioflavin T (ThT) is a classic amyloid dye that is commonly used to probe amyloid-beta fibril formation because of its strong fluorescence emission upon binding to amyloid fibril structures [134, 136]. A ThT stock solution was prepared mixing 8 mg of ThT in 10 mL of PBS buffer. This solution was filtered through a 0.20 µm syringe filter and the stock solution was diluted in buffer (1:50 ratio). 50 µM of Aβ(1–42) peptide was incubated at 37 °C in 96 well plates with different conditions: 30 µM quercetin, loaded nanoparticles and unloaded nanoparticles. Finally, ThT solution (0.7 mg/mL) was added to each well and the fluorescence intensity was measured every 30 minutes during 24 hours using a Biotek Synergy 2 fluorescence spectrometer (Winooski, Vermont, USA). ThT conjugated with fibrils has excitation at 450 nm and maximum emission at 482 nm [137].

2.16. STATISTICAL ANALYSIS

Statistical analysis was performed using SPSS software (v 24.0; IBM, Armonk, NY, USA). The measurements were repeated three times and data were expressed as mean ± SD. Data were analyzed using one-way analysis of variance (one-way ANOVA), followed by Bonferroni, Tukey and Dunnett post-hoc tests. A p value lower than 0.05 was considered statistically significant.

CHAPTER 3. RESULTS AND DISCUSSION

3.1 ^{1}H-NMR CHARACTERIZATION OF TRANSFERRIN-FUNCTIONALIZED CONJUGATE

The coupling of transferrin to DSPE-PEG-NH_2 was confirmed by ^{1}H-NMR (Figure 7). In the spectrum of DSPE-PEG-Transferrin, it is possible to find several characteristic peaks of DSPE, PEG_{2000} repetitions and transferrin protein. The proton peaks at 0.85 ppm (CH_3), 1.30 ppm (CH_2) and 4.25 ppm (PO_4CH_2CH) are attributed to DSPE phospholipid [138]. At 3.75 ppm one can observe the peak that corresponds to CH_2CH_2O on PEG_{2000} repetitions [138], while the peak at 2.10 ppm confirms the presence of transferrin amino groups in DSPE-PEG-Transferrin spectrum [123, 139]. Additionally, the presence of proton peaks of transferrin at 0.80 to 1.30 ppm also contributes to the baseline rising in the conjugate spectra [140]. In fact, the spectrum of DSPE-PEG-Transferrin seems to be a mixture of peaks from both DSPE-PEG-NH_2 plus transferrin spectra. However, the intensity of peaks have decreased, suggestion the attachment of transferrin to the DSPE-PEG_{2000} moiety and indicating the successful functionalization

3.2. ^{1}H-NMR CHARACTERIZATION OF RVG29-FUNCTIONALIZED CONJUGATE

Figure 8 shows the ^{1}H NMR spectra resulted from the coupling of RVG29 peptide to DSPE-PEG-MAL. In the spectrum of DSPE-PEG-MAL, one can observe characteristic peaks of DSPE, PEG2000 repetitions and the maleimide group. The proton peaks at 0.85 ppm (CH_3), 1.30 ppm (CH_2), 1.60 ppm (CH_2CH_2CO), 2.35 ppm (CH_2CO) and 4.25 ppm (PO_4CH_2CH) are attributed to DSPE phospholipid [141, 142]. At 3.75 ppm it is possible to visualize the CH_2CH_2O peak of the repeat units of PEG_{2000} [141, 142], while the peak at 6.70 ppm confirms the presence of the maleimide group in DSPE-PEG-MAL spectrum [141-143]. After functionalization with RVG29, the peaks which correspond to DSPE and PEG_{2000} remain in the NMR spectrum of DSPE-PEG-RVG29. However, the maleimide peak at 6.70 ppm completely disappeared, indicating the successful addition between the maleimide group of DSPE-PEG-MAL and the thiol

moieties of RVG29 [141-143]. Besides, it is possible to observe a peak at 2.10 ppm related to the presence of RVG29 amino groups and also the characteristic peaks of aromatic protons of RVG29 amino acids at 6.00 to 7.60 in the ^{1}H NMR spectrum of DSPE-PEG-RVG29 conjugate. Therefore, the NMR spectra proved the successful functionalization of DSPE-PEG$_{2000}$ with RVG29 peptide.

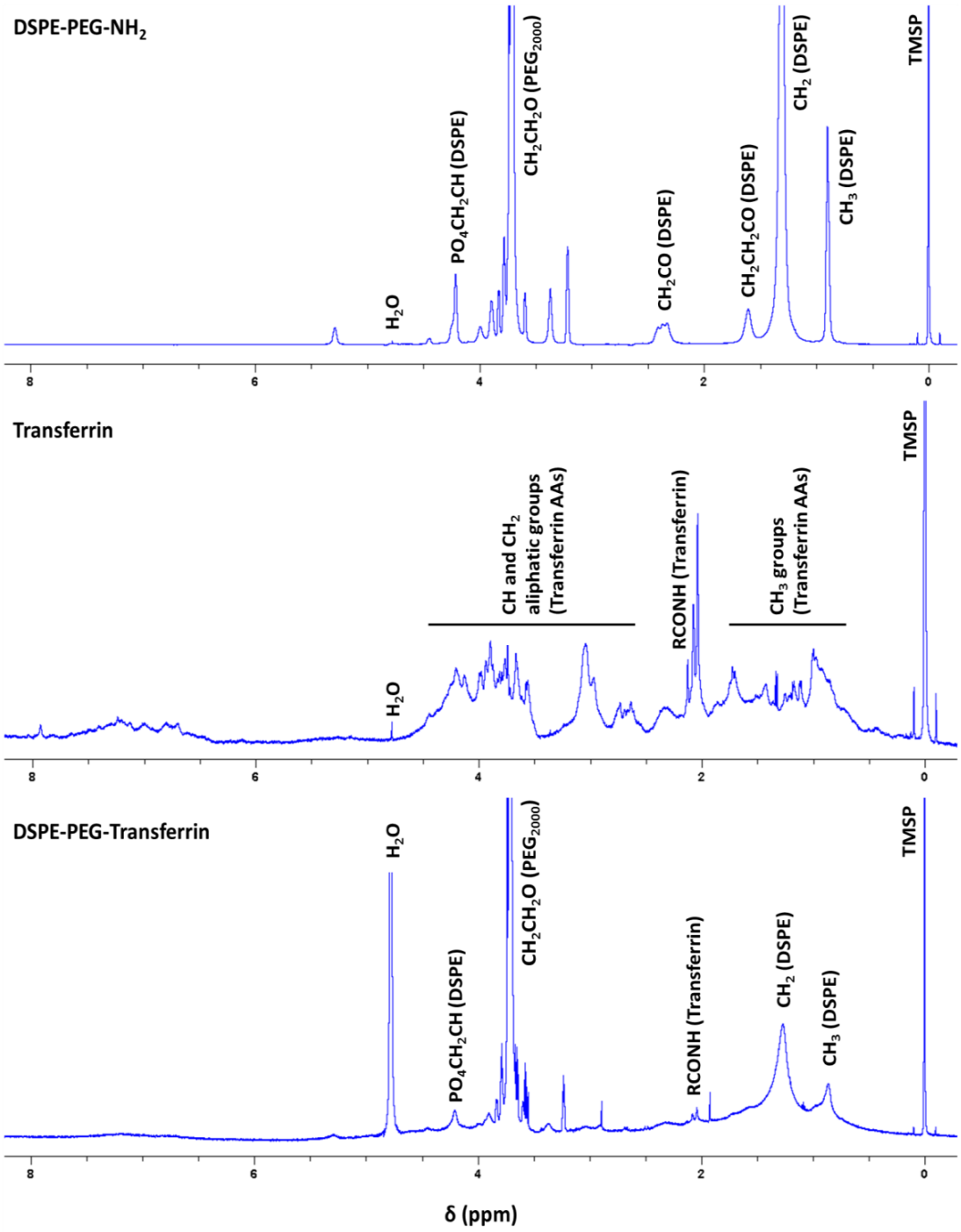

Figure 7. ^{1}H NMR spectra of DSPE-PEG-NH$_2$, Transferrin and DSPE-PEG-Transferrin samples.

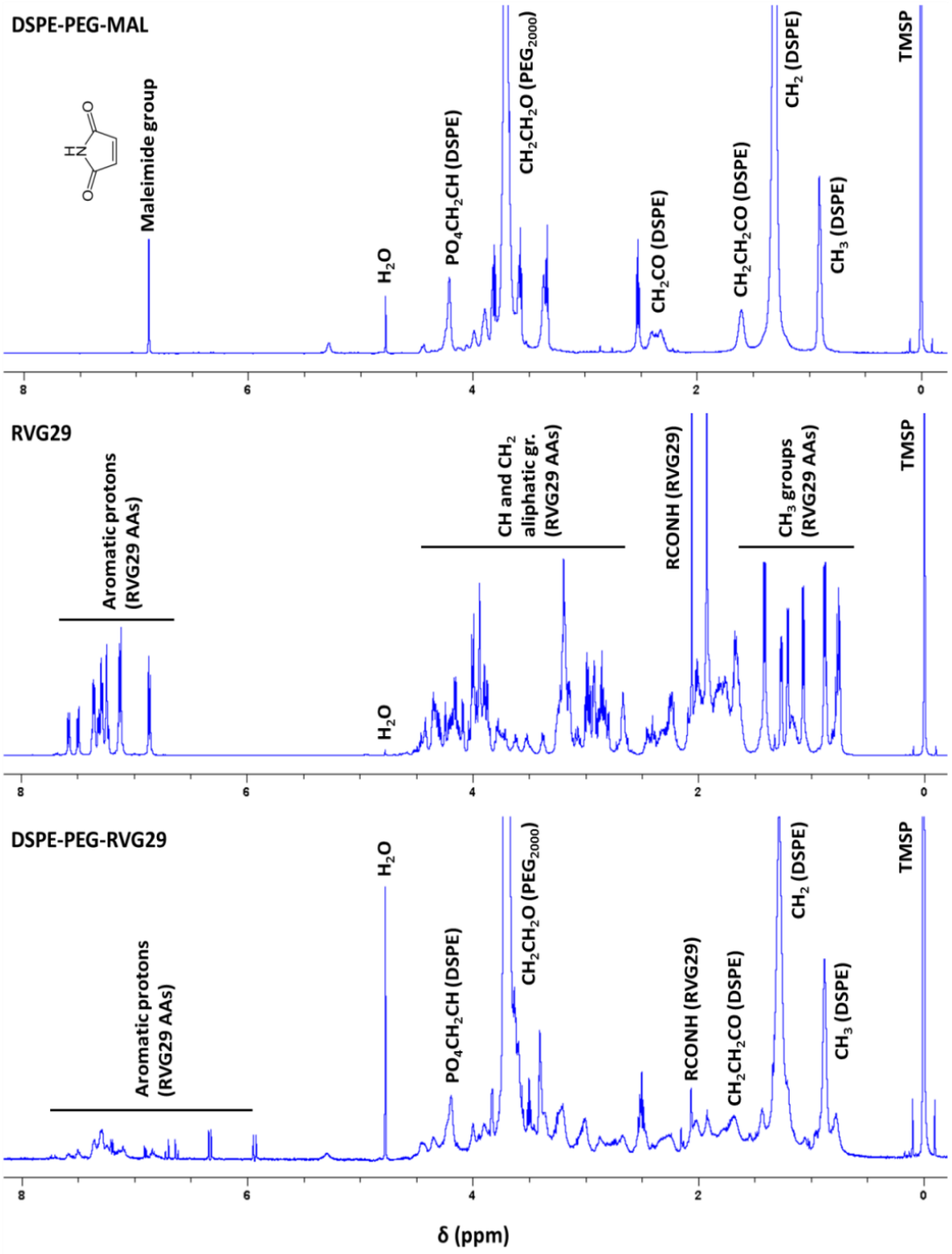

Figure 8. ^{1}H NMR spectra of DSPE-PEG-MAL, RVG29 and DSPE-PEG-RVG29 samples.

3.3. FT-IR CHARACTERIZATION OF TRANSFERRIN- AND RVG29-FUNCTIONALIZED NANOPARTICLES

The functionalization with Transferrin and RVG29 peptide was confirmed by infrared spectra analysis of both functionalized and non-functionalized nanoparticles. Infrared

spectra result from transitions between quantized vibrational energy states and molecular vibrations are characteristic of specific functional groups. This thecnique use the infrared radiation to excite molecules and make them vibrate. Every functional groups need a specific energy to vibrate and it is possible to identify what groups correspond to each band in the FT-IR spectra [144]. The nanoparticles have been previously lyophilized because the signal from -OH groups could hide other important and characteristic functional group peaks. The spectra obtained are depicted in Figure 9 and 10.

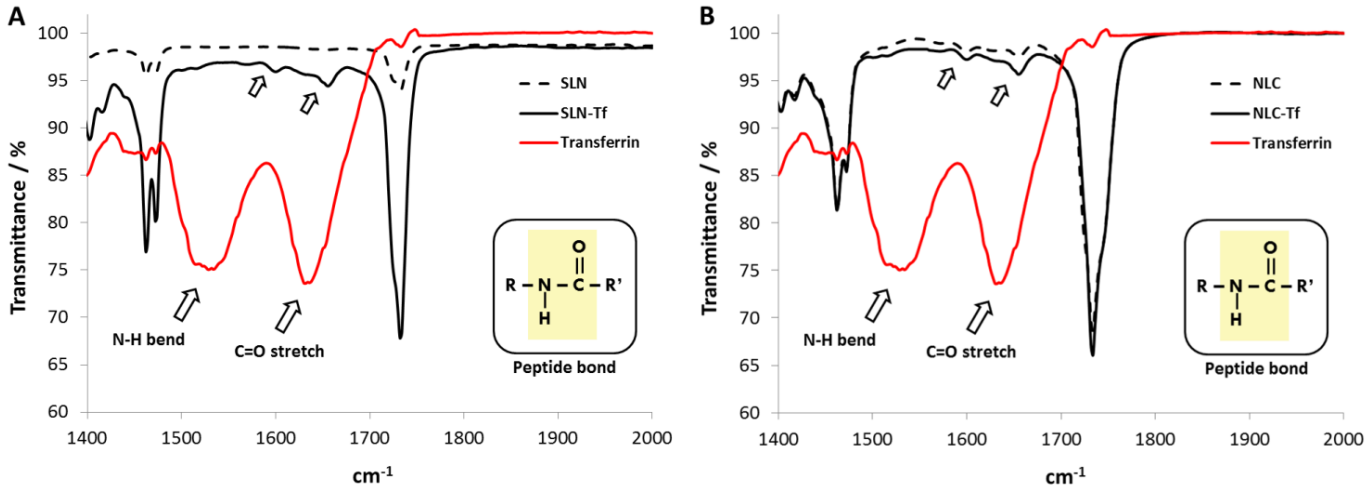

Figure 9. Infrared spectra obtained by FT-IR for SLN (A) and NLC (B) before and after functionalization with transferrin protein. **Note:** Transferrin sample was used as a reference to compare with the functionalized nanoparticles.

In Figure 9, one can find two main bands in transferrin reference sample that also appear in Tf-functionalized nanoparticles spectra. These bands match to the N-H bending vibrations (1550 cm^{-1}) and C=O stretching vibrations (1650 cm^{-1}) present in the peptide bonds between amino acids of transferrin protein. In Figure 10, besides the previously mentioned bands that also appear in RVG29 reference sample, one can additionaly visualize a band that corresponds to the N-H stretching vibrations (3300 cm^{-1}) that is also present in the RVG29-functionalized nanoparticles spectra [145]. Therefore, it was possible to see characterisitic bands from the peptide bond in all FT-IR spectra, indicating that nanoparticles were successfully functionalized. These data is in agreement with the NMR results, bringing strong evidences for nanoparticles functionalization.

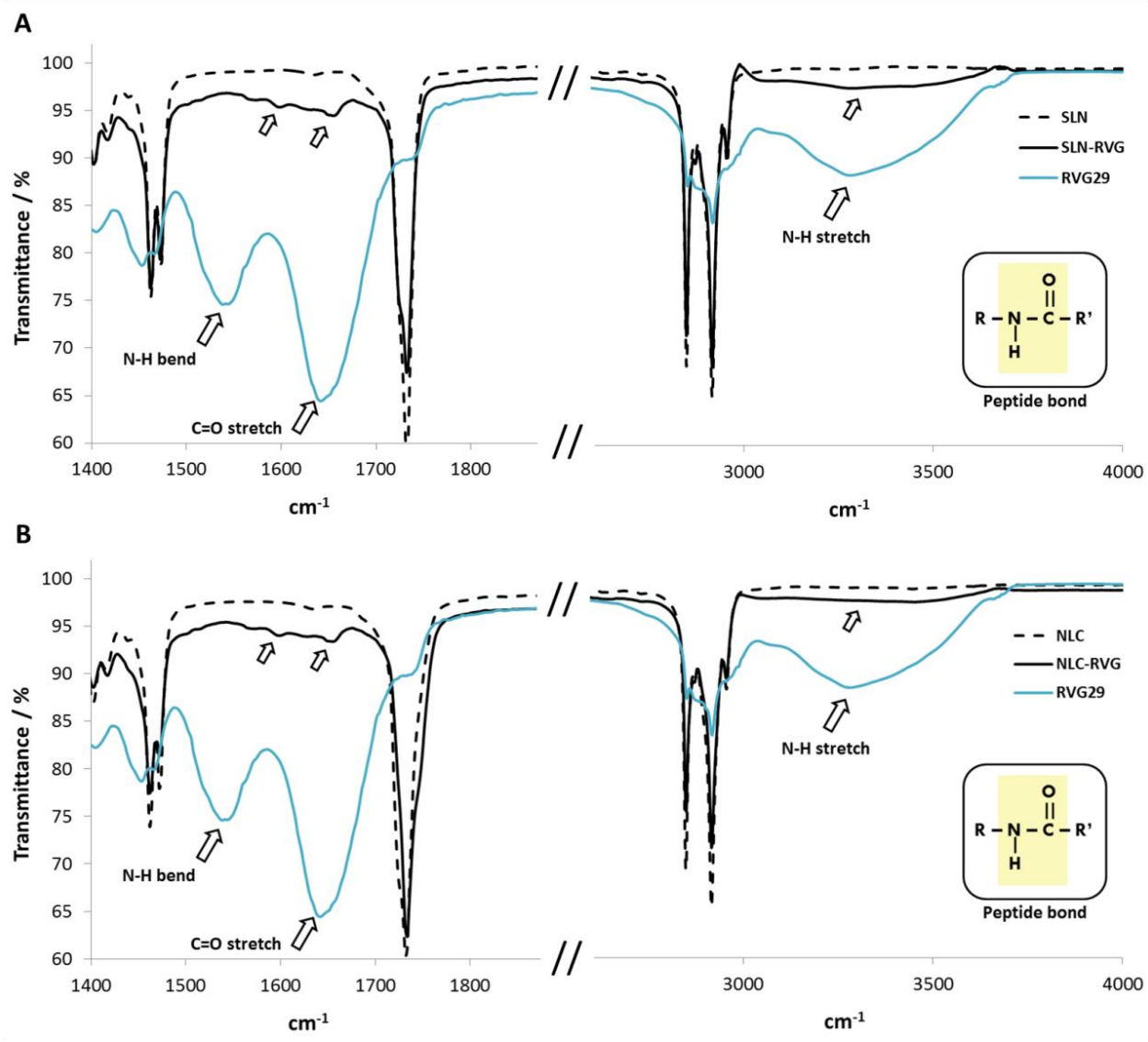

Figure 10. Infrared spectra obtained by FT-IR for SLN (A) and NLC (B) before and after functionalization with RVG29 peptide. **Note:** RVG29 sample was used as a reference to compare with the functionalized nanoparticles.

3.4. MORPHOLOGY DETERMINATION

Observing the images obtained by TEM (Figure 11), both types of nanoparticles (SLN and NLC) showed a spherical and uniform morphology and smooth surfaces. The images also revealed no visible aggregation of particles which is a good indicator of the stability of formulations. The encapsulation of quercetin did not apparently modify the nanoparticles morphology, as well as the functionalization of nanoparticles with transferrin or RVG29 ligands. This ensured that the functionalization with transferrin or

RVG29 peptide did not influence the morphology and stability of particles. However, it is not possible to distinguish by TEM analysis any morphological or structural difference between SLN and NLC nanoparticles, neither between particles before and after quercetin encapsulation or ligands functionalization.

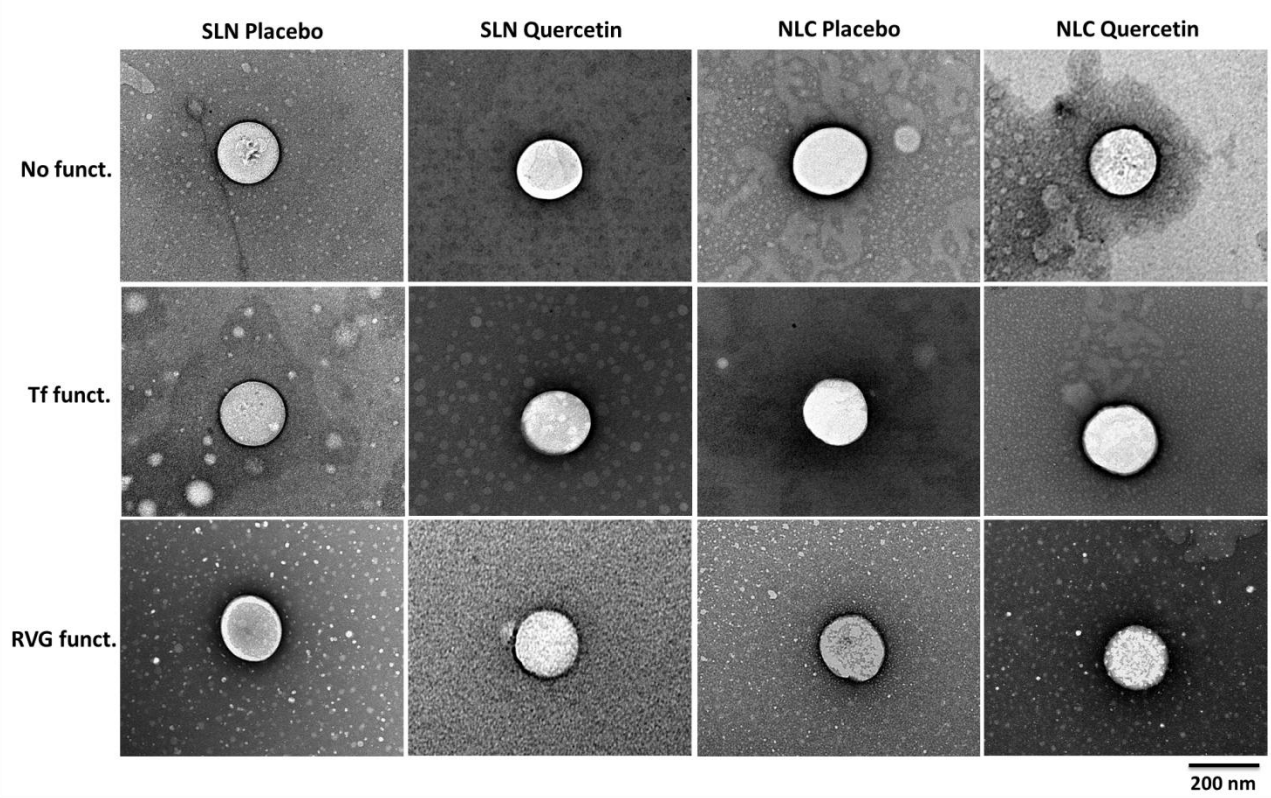

Figure 11. Transmission electron microscopy images of lipid nanoparticles: non-functionalized (upper side), transferrin-functionalized (midle) and RVG29-functionalized nanoparticles (lower side).

3.5. PHYSICOCHEMICAL CHARACTERIZATION AND STABILITY STUDY OF NANOPARTICLES

3.5.1. PARTICLE SIZE MEASUREMENTS

The size of nanoparticles is an important factor which determines if the nanosystems can cross certain biological barriers, such as BBB [146]. It is also crucial to analyze the nanoparticles size in order to predict their biodistribution, accumulation and elimitation.

With this in mind, the hydrodynamic diameter was measured by DLS (Table 6) and this study was also conducted over time in order to evaluate the stability of nanoparticles (Figure 12). All nanoparticles showed a size lower than 250 nm which is an important characteristic that enables the permeation through the BBB [146]. These results are in agreement with TEM images where it was possible to observe nanoparticles with an average size around 200 nm. NLC were found to be slightly lower than SLN ($p<0.05$), while the presence of quercetin showed to increase the mean average size of both types of lipid nanoparticles ($p<0.05$), except for RVG29-functionalized nanoparticles (Table 6).

Table 6. Characterization of non-functionalized and functionalized lipid nanoparticles with transferrin and RVG29 according to their size, polydispersity index, zeta potential and quercetin entrapment efficiency.

Formulation code	Particle size (nm)	Polydispersity index	Zeta potential (mV)	Entrapment efficiency (%)
SLN Placebo	166.9±5.9	0.13±0.02	-31.4±5.5	-
SLN Quercetin	194.9±4.2 *	0.09±0.02	-31.3±5.2	81±12
NLC Placebo	146.7±4.5	0.05±0.01	-24.4±1.5	-
NLC Quercetin	170.3±4.7 *	0.12±0.03	-27.8±2.3	97±10
SLN-Tf Placebo	198.6±24.5	0.09±0.01	-35.2±3.2	-
SLN-Tf Quercetin	233.8±18.4 *	0.06±0.01	-31.8±7.7	77±11
NLC-Tf Placebo	174.0±10.1	0.07±0.03	-24.9±7.2	-
NLC-Tf Quercetin	219.3±12.6 *	0.08±0.12	-27.6±1.8	81±6
SLN-RVG Placebo	246.3±29.1	0.09±0.03	-25.8±6.6	-
SLN-RVG Quercetin	201.4±22.6	0.13±0.07	-20.3±7.0	84±10
NLC-RVG Placebo	223.7±4.5	0.07±0.05	-24.2±0.9	-
NLC-RVG Quercetin	122.2±21.6 *	0.23±0.08 *	-24.5±2.5	93±2

Note: All values represent the mean ± standard deviation (n = 3). * denotes statistically significant differences when compared to placebo nanoparticles ($P<0.05$).

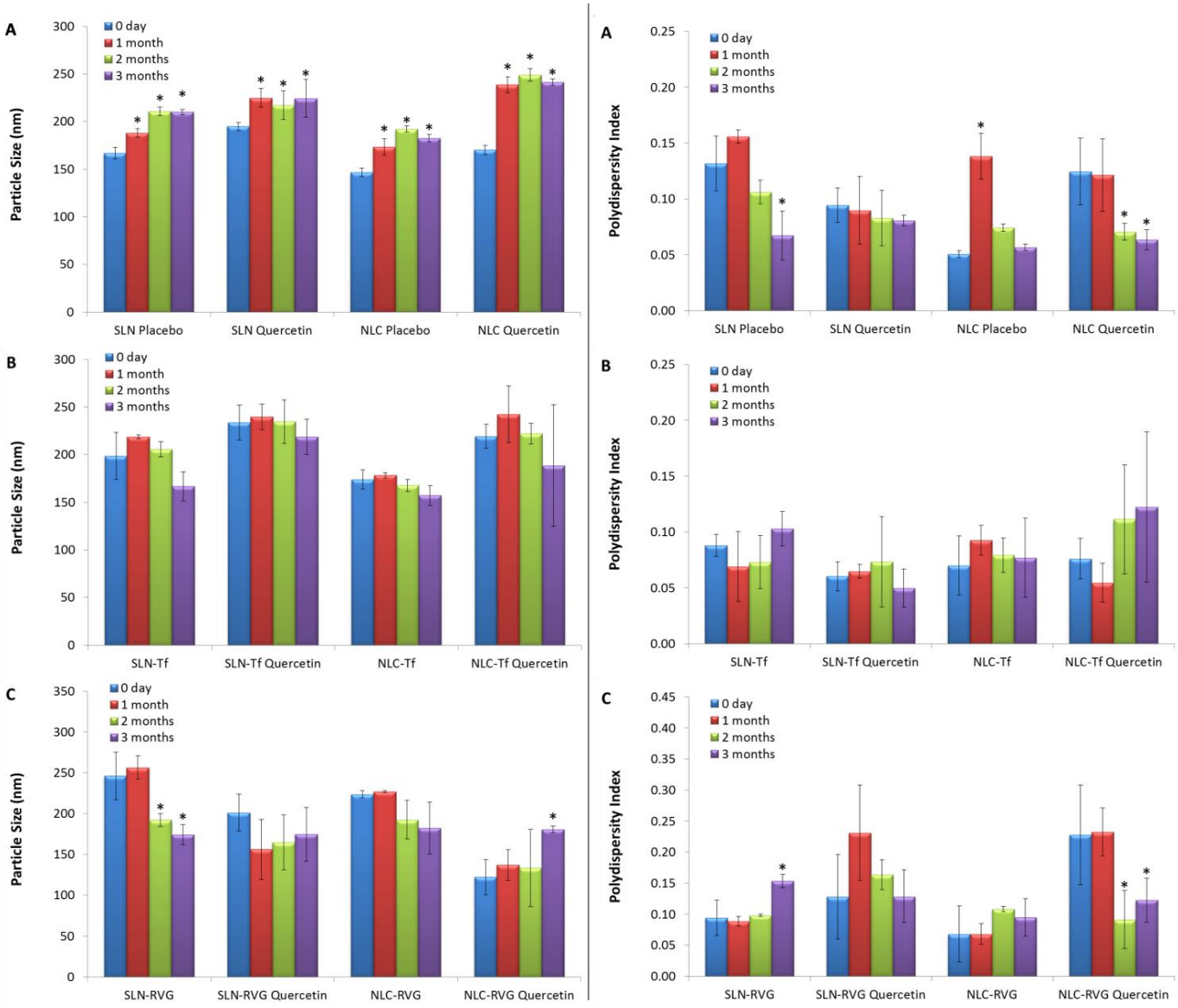

Figure 12. Effect of time of storage on particle size (left side) and polydispersity index (right side) of lipid nanoparticles: (A) non-functionalized nanoparticles; (B) transferrin-functionalized nanoparticles; and (C) RVG29-functionalized nanoparticles. All data represent the mean ± standard deviation (n = 3). * denotes statistically significant differences when compared to day 0 (P<0.05).

Polydispersity index is another important factor to be evaluated, which indicates the width of the particle size distribution. In fact, we are interested in a monodispersed distribution of sizes, because one can ensure that almost all nanoparticles have the ideal size for our application, in this case to cross BBB. In Table 6, it is possible to see that polydispersity index was lower than 0.2 for all formulations, suggesting a homogeneous size distribution with low variability of sizes and no aggregation. Concerning the stability study over time (Figure 12), it is important to note that almost all functionalized and non-functionalized nanoparticles maintained their low polydispersity below 0.2, with the exception of quercetin-loaded RVG29-nanoparticles

that showed slightly larger size distributions, but still have acceptable monodispersity, with low variability and no aggregation. In fact, this type of distribution is usual in SLNs and NLCs made using the high shear homogenization and ultrasound method, as it is very difficult to achieve a unimodal distribution of sizes.

3.5.2. ZETA POTENTIAL MEASUREMENTS

Another extremely important tool consists in measuring the zeta potential of nanoparticles. This parameter allows us to study the stability of the nanoparticles in solution since it tells us if nanoparticles have the tendency to form aggregates. As a result of the application of an external electrical field, the particles will have a certain mobility according to their surface charge. If the absolute value of zeta potential of nanoparticles is higher than 30 mV this will induce stronger repulsive forces between particles and thereby it will lead to a greater stability of the colloidal dispersions [147]. The results revealed an average zeta potential around -30 mV for all formulations, indicating a rather high value to prevent aggregation of nanoparticles (Table 6). At the same time, the presence of quercetin did not change zeta potential of neither SLN nor NLC ($p>0.05$).

Additionally, zeta potential values remained higher than 30 mV in all non-functionalized and transferrin-functionalized formulations after three months of storage showing that particles will not form aggregates over time which is important to ensure the stability of the colloidal dispersions (Figure 13). These results are in agreement with TEM images where no particle aggregation was observed.

Concerning RVG29-functionalized nanoparticles, zeta potential was in general between -20 mV and -25 mV and remained almost unchanged along three months of study. These values were lower than for non-functionalized and transferrin-nanoparticles, but this was not an intrinsic property of RVG29-nanoparticles. In fact, this difference derived from the fact that RVG29 formulations were not synthezised in water but instead in PBS, to ensure the stability of thioether bound between RVG29 peptide and the maleimide group. As a consequence, the ions present in PBS may reduce the nanoparticles superficial charge, thereby decreasing the values of measured zeta potential.

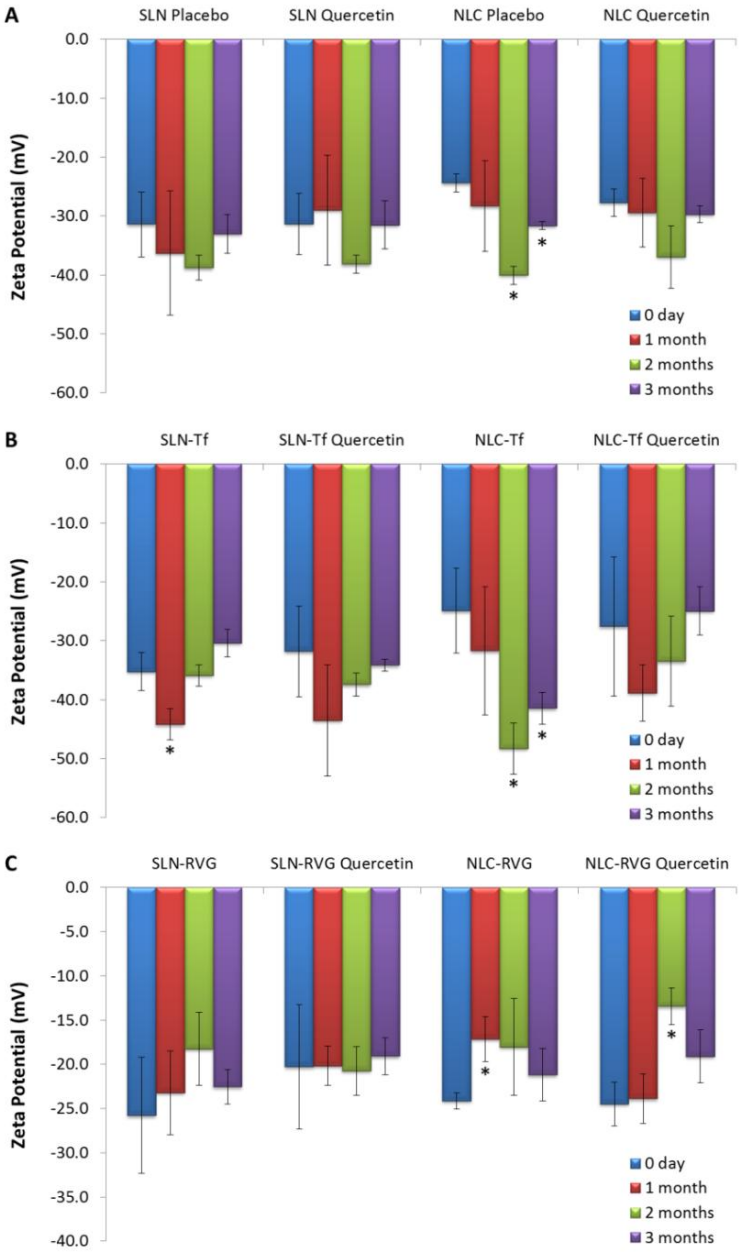

Figure 13. Effect of time of storage on zeta potential of lipid nanoparticles: (A) non-functionalized nanoparticles; (B) transferrin-functionalized nanoparticles; and (C) RVG29-functionalized nanoparticles. All data represent the mean ± standard deviation (n = 3). * denotes statistically significant differences when compared to day 0 ($P<0.05$).

3.5.3. QUERCETIN ENTRAPMENT EFFICIENCY

Encapsulation efficiency is also an important parameter in order to ensure the delivery of the desired amount of quercetin into the brain, while keeping to a minimum the number of lipid nanoparticles used. In fact, if particles are only able to encapsulate a low quantity of quercetin it will be necessary to administrate more nanoparticles and

this may bring problems related with thrombus formation [148]. The results revealed that both SLN and NLC are able to encapsulate high amounts of quercetin (Table 6). A value of entrapment efficiency around 80-90% corresponds to 8-9 mg of quercetin entrapped inside the nanoparticles which is quite high. It is also possible to notice that NLC have a tendency to incorporate higher quercetin amounts than SLN, probably due to less ordered crystalline structure of NLC with small cavities in the lipid matrix that may allow a better accommodation of quercetin [149, 150].

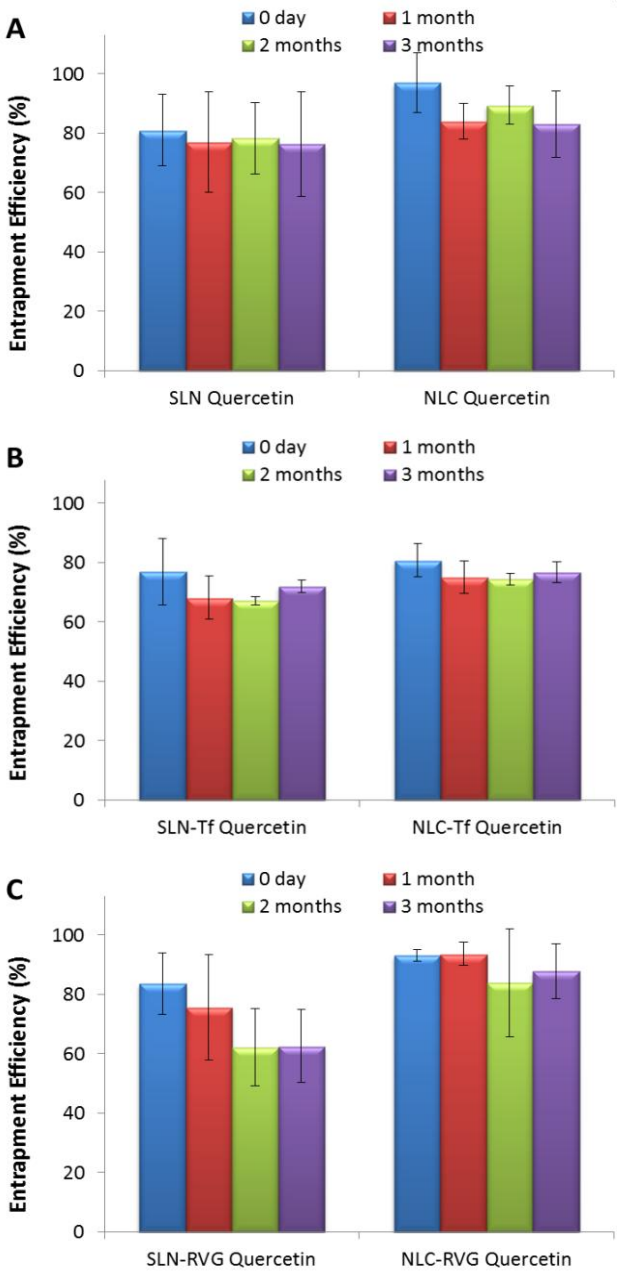

Figure 14. Effect of time of storage on quercetin entrapment efficiency of lipid nanoparticles: (A) non-functionalized nanoparticles; (B) transferrin-functionalized nanoparticles; and (C) RVG29-functionalized nanoparticles. All data represent the mean ± standard deviation (n = 3). * denotes statistically significant differences when compared to day 0 ($P<0.05$).

The stability study over time suggested that almost all encapsulated quercetin remained inside lipid nanoparticles after 3 months, both non-functionalized and functionalized ones (Figure 14). However, despite not being statistically significant, a slight tendence for the encapsulated flavonol to decrease after three months in SLN-RVG29 can be assumed. This fact can be justified by the highly ordered crystalline structure of SLN which may trigger a premature release over time. Eventhough, this entrapment decrease is not so evident and SLN-RVG still have a lot of compound associated with the nanoparticles.

3.6. QUERCETIN PHOTOSTABILITY STUDY

The present photostability study was very important to investigate the protection effect of lipid nanoparticles against photodegradation of quercetin. Figure 15A displays the absorption intensity spectra of quercetin before and after UV light exposure during 6 h. The result for free quercetin is in agreement with a previous study which shows a decrease in the compound absorption intensity at 373 nm [19]. In fact, quercetin photosensitivity is well documented in alcoholic solutions after UVA lamp exposure [19]. Therefore, the ability of lipid nanoparticles to protect the compound against photodegradation was further investigated and the absorption spectra for quercetin loaded in SLN and NLC after UV irradiation are also represented in Figures 15A. The results suggest that both types of lipid nanoparticles (SLN and NLC) reduced photodegradation profile. In fact, around 55% of quercetin in solution was photodegraded after UV exposure, while the entrapped compound inside lipid nanoparticles showed only around 10% of degradation (Figure 15B). From these results, it is possible to conclude that nanoparticles protected quercetin from photodegradation. At the same time, this was an indirect way of proving that quercetin was really entrapped inside nanoparticles, because only free compound suffers degradation. Therefore, if almost none quercetin was photodegraded after UV light esposure, this means that quercetin was actually encapsulated inside lipid matrix of nanoparticles.

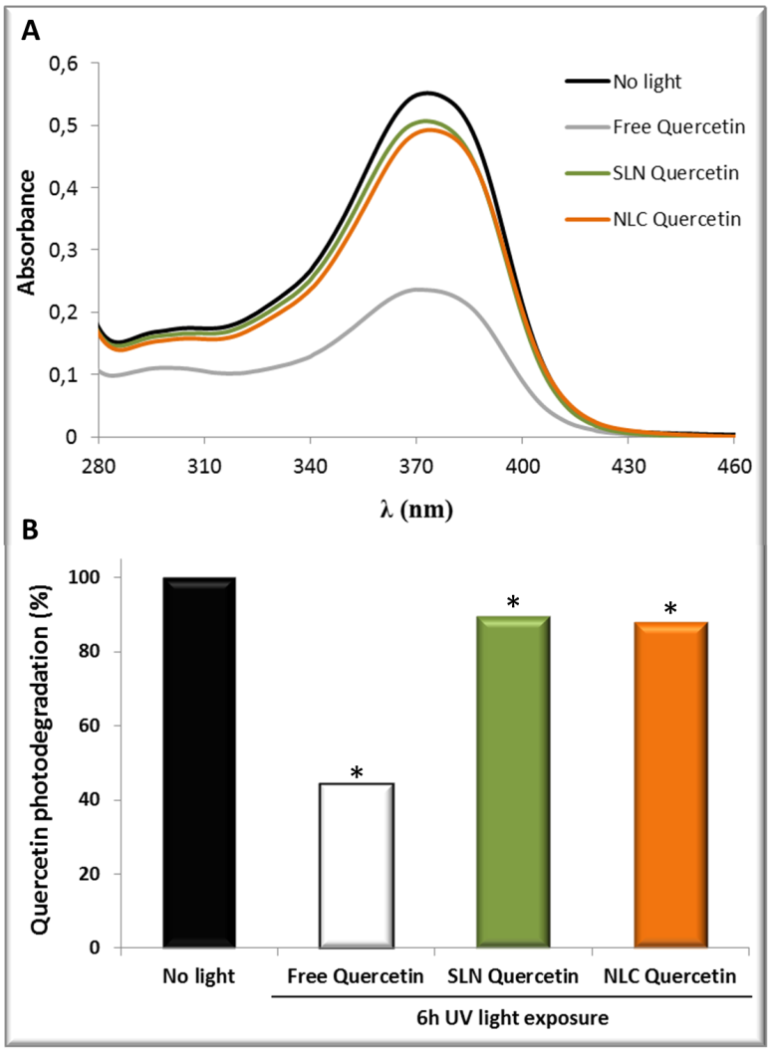

Figure 15. Photostability study of free quercetin exposed to UV light for 6 hours compared to quercetin-loaded SLN and NLC. (A) absorption spectra; (B) photodegradation profile. * denotes statistically significant differences when compared to sample with no light treatment ($P<0.05$).

3.7. CYTOTOXICITY STUDY

In order to validate the developed nanosystems as a secure approach to deliver quercetin in the brain, LDH assay was conducted in hCMEC/D3 cells to evaluate potential cytotoxicity of quercetin-loaded nanosystems. This technique allows the quantification of lactate dehydrogenase (LDH) that is released from cells to cell culture medium when cell membrane is damaged [151]. This enzyme reduces NAD^+ into NADH, being tetrazolium salt INT consequently reduced into a red formazan product [152]. The extension of this reaction can be monitored by measuring absorbance and this is proportional to cell death levels. Figure 16A and B compares cytotoxicity of non-functionalized nanoparticles to transferrin-functionalized or RVG29-functionalized ones, respectively. In general terms, it is possible to see that cytotoxicity was lower than 30%

for any type of nanoparticles, even for the highest concentration tested (30 µM) which was the maximum concentration used in the subsequent *in vitro* validation tests. Therefore, no relevant cytotoxic effects were observed for the concentration used in the permeability studies, indicating that nanoparticles did not considerably affect membrane integrity. In fact, both transferrin- and RVG29-nanoparticles showed very low cytotoxicity values, not exceeding 25% and 15%, respectively, ensuring their safety.

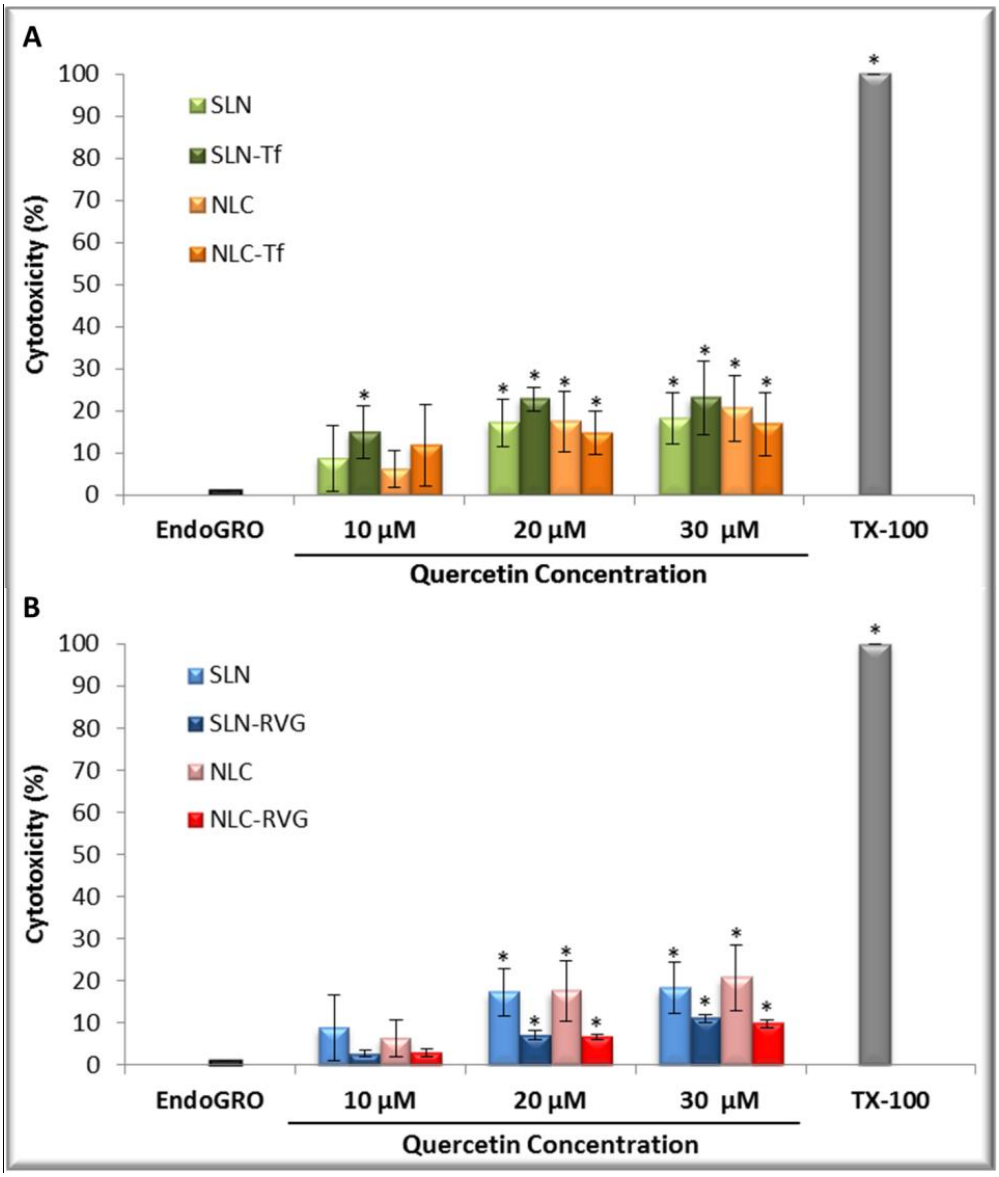

Figure 16. hCMEC/D3 cytotoxicity assessed by LDH assay when exposed to quercetin-loaded SLN and NLC. (A) transferrin-functionalized study; (B) RVG29-functionalized study. All values represent the mean ± standard deviation (n = 3). * denotes statistically significant differences (P<0.05) when compared to EndoGRO medium which represents the minimum cytotoxicity.

3.8. BBB PERMEABILITY STUDY

hCMEC/D3 cell monolayer is a commonly used BBB model system, since it exhibits permeability values well correlated with *in vivo* permeation across human BBB [129, 130]. Therefore, in the present study hCMEC/D3 cells were cultured in transwell devices and permeability studies were carried out to test the capacity of the developed nanoparticles to cross BBB. Due to quercetin low solubility, the permeability of free quercetin in solution was not possible to investigate since we had no way of reproducing these conditions nor to quantify the free compound experimentally. The permeability profiles of non-functionalized nanoparticles compared to transferrin-functionalized or RVG29-functionalized nanoparticles after 4 hours assay are depicted in Figure 17A and B, respectively. In a first glance, it was possible to observe a gradual increase of all nanoparticles content in the basolateral side of cell monolayer over time, showing that nanoparticles were progressively permeating the BBB barrier. From the analysis of Figure 17A, one can conclude that NLC had statistically significant higher permeabilities compared to SLN, both for non-functionalized or funtionalized nanoparticles. However, it is important to note that transferrin-nanoparticles did not significantly increase BBB permeability compared to non-functionalized nanoparticles, which may indicate the saturation of the receptor-mediated transport of transferrin over hCMEC/D3 cell monolayer. In fact, it is well reported on the literature that the concentration of endogenous transferrin is sometimes high leading frequently to a saturation of the protein binding sites on the BBB receptor and hindering the receptor-mediated active permeability of transferrin-functionalized nanoparticles [153]. Regarding Figure 17B, once again it was easy to conclude that NLC permeability was greater than SLN. Furthermore, a significant increase on RVG29-nanoparticles permeability (1.5-fold higher) was observed when compared to non-functionalized nanoparticles, for both SLN and NLC systems. In fact, some works report that RVG29 peptide can binds to nicotinic acetylcholine receptors (nAchR) that are expressed in the BBB, enabling the crossing of this barrier [154]. Besides, the expression of nAchR alpha7 on hCMEC/D3 cells has been also confirmed by realtime PCR [155]. Therefore, it is possible to state that RVG29 conjugation to nanoparticles really enhances *in vitro* permeability through the BBB which might lead to an increase of quercetin brain delivery *in vivo*.

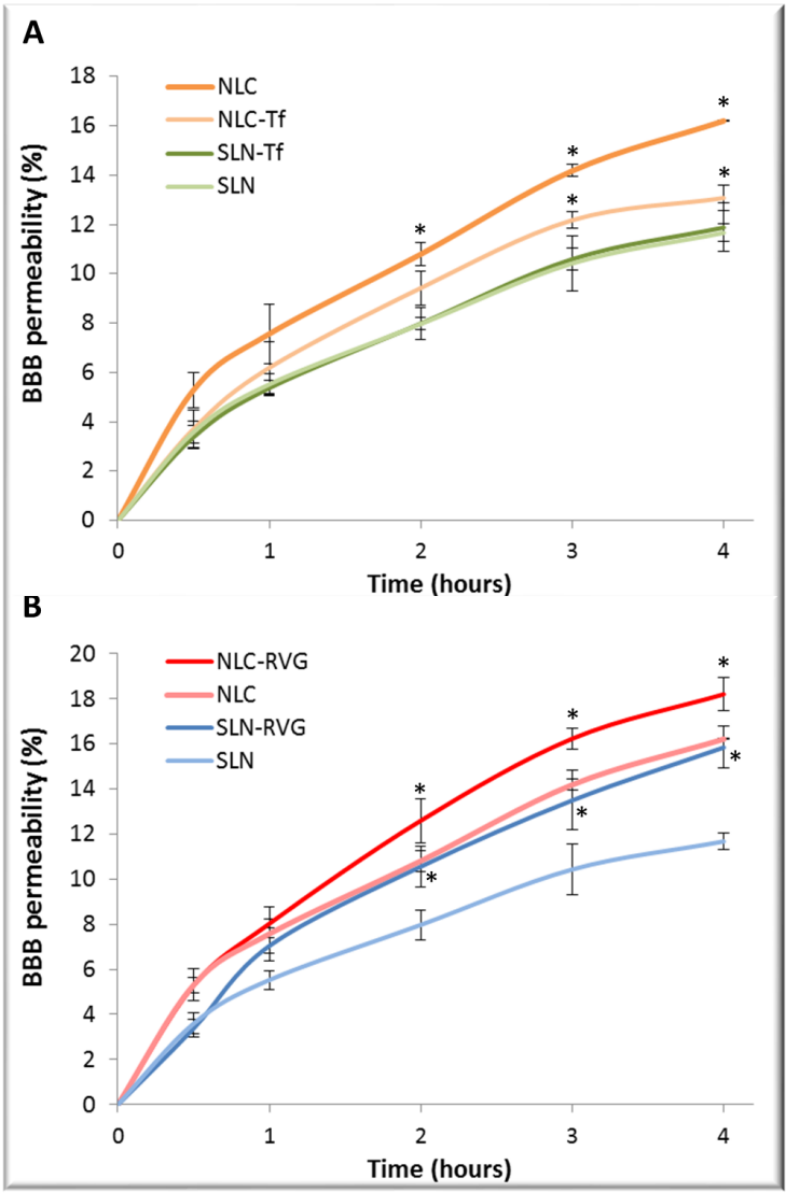

Figure 17. Permeability profile of nanoparticles across hCMEC/D3 cell monolayer over 4 hours, mimicking BBB transport conditions. (A) transferrin-functionalized study; (B) RVG29-functionalized study. All values represent the mean ± standard deviation (n = 3). * denotes statistically significant differences (P<0.05) when compared to the respective non-functionalized nanoparticles.

3.9. AMYLOID-BETA PEPTIDE STUDY

3.9.1. IMPACT OF QUERCETIN AND NANOPARTICLES ON AB(1-42) FIBRILLATION

The final purpose of this work was to stablish a nanosystem capable of delivering quercetin in brain to take advantage of the neuroprotective properties of this compound. There are evidences in the literature for the ability of quercetin to inhibit fibril formation which result from the aggregation of amyloid-beta peptide and that is in

the origin of Alzheimer's diseases [73]. In order to test the effect of quercetin and nanoparticles on Aβ(1-42) peptide fibrillation, a ThT binding assay was performed. ThT is a poor fluorophore in solution, but in the presence of β-sheet fibrils, ThT can enter into cavities produced by the quaternary structure of the protein and the rotation becomes restricted which results in an increase in fluorescence quantum yield. Therefore, the intensity of fluorescence is proportional to the amyloid fibrils formation [134, 136, 137]. However, if the fluorescence intensity of ThT significantly decreases in the presence of a compound, one can conclude that there is an inhibition effect of peptide fibrillation.

The interaction of quercetin and nanoparticles with the amyloid-beta peptide after 24h of incubation at 37 °C can be interpreted from Figure 18. It is possible to conclude that quercetin decreased the fluorescence intensity of ThT when compared to Aβ(1-42) peptide alone, which indicates that fibrils formation was attenuated by this compound, corroborating the study of Kim et al. [73]. By the other hand, unloaded SLN and NLC seem to promote the aggregation of amyloid-beta peptide because fluorescence intensity increases, corresponding to ThT binding to the β-sheet amyloid fibrils. In fact, this result is is agreement with some previous studies reported in literature where lipid nanoparticles acted as nuclei of aggregation, promoting peptide fibrillation [156-158].

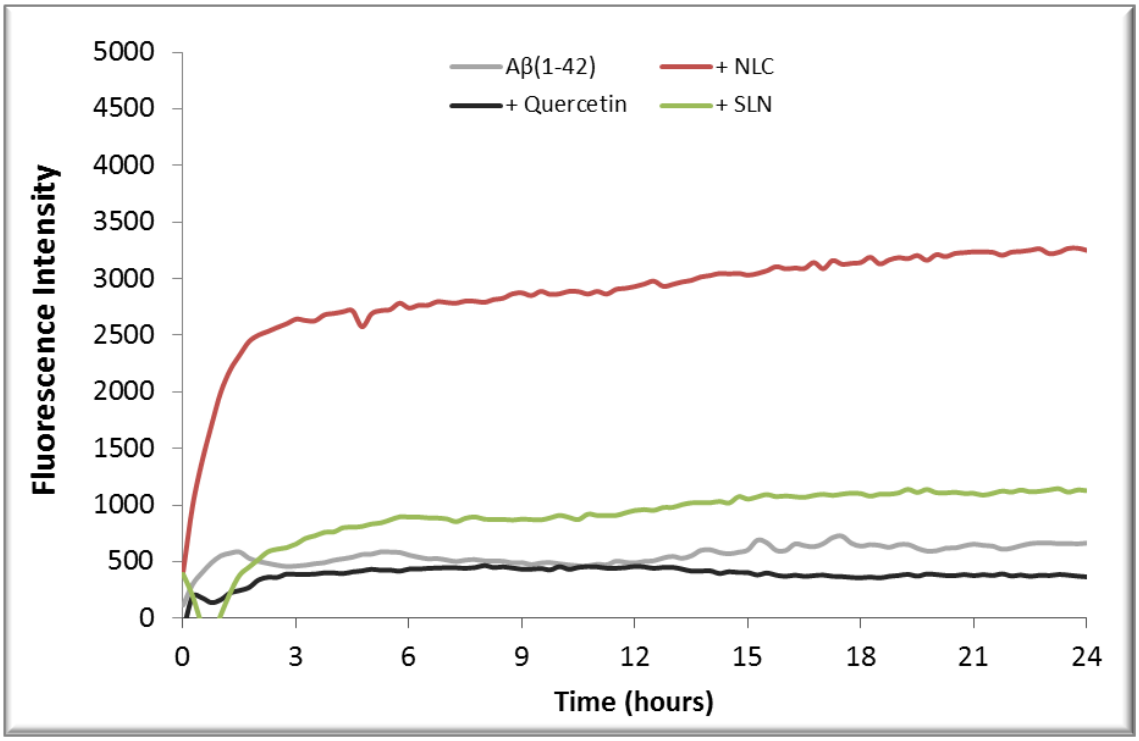

Figure 18. Fluorescence intensity of ThT in Aβ(1-42) samples alone or containing free quercetin, NLC or SLN, over 24h of incubation at 37 °C.

3.9.2. IMPACT OF QUERCETIN ENCAPSULATED IN NANOPARTICLES ON AB(1-42) FIBRILLATION

Figure 19 summarizes the effect of different quercetin-loaded nanoparticles on Aβ(1-42) fibrillation when compared to free quercetin and unloaded nanoparticles. Actually, after encapsulated in lipid nanoparticles, quercetin seemed to counteract the tendency for fibrillation caused by unloaded SLN and NLC, previously reported as nuclei of aggregation. In fact, both quercetin-loaded SLN and NLC were capable of decreasing fluorescence intensity, inhibiting fibril formation when compared to unloaded SLN and NLC, indicating that the presence of quercetin could dissipate the aggregation promoting effect of nanoparticles.

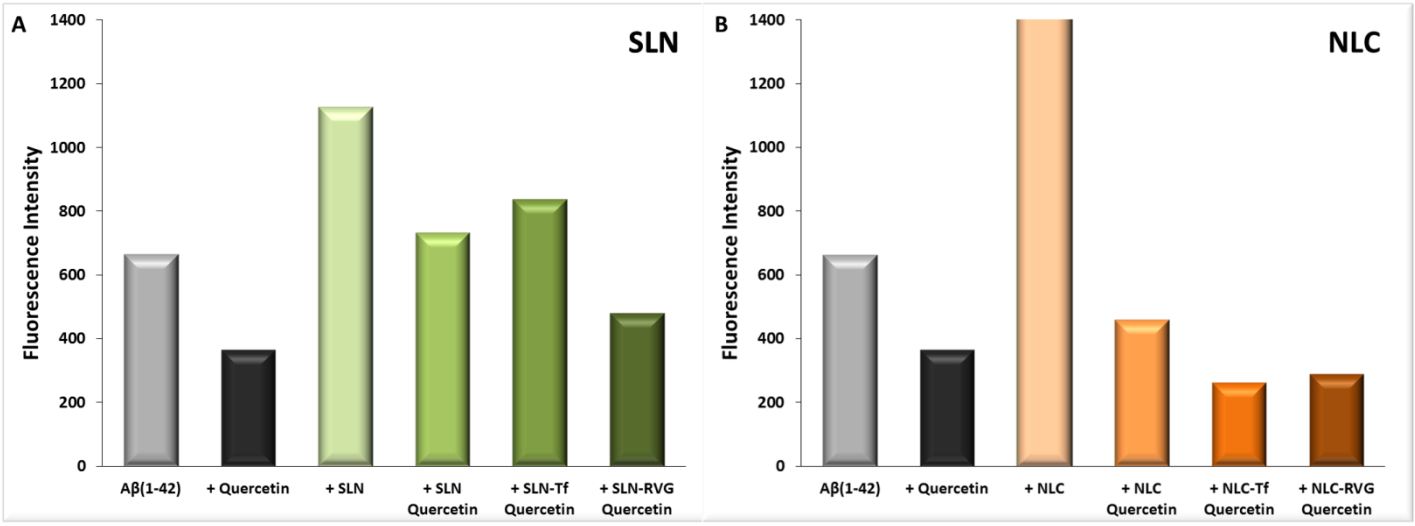

Figure 19. Fluorescence intensity of ThT in Aβ(1-42) samples alone or containing free quercetin, unloaded nanoparticles and quercetin-loaded functionalized or non-functionalized nanoparticles, after 24h of incubation at 37 °C: (A) SLN study; and (B) NLC study. * denotes statistically significant differences ($P<0.05$) when compared to Aβ(1-42) sample alone.

In Figure 19B, it is possible to notice that all quercetin-loaded NLC (both non-functionalized and functionalized with transferrin and RVG29) were able to inhibit peptide aggregation when compared to Aβ(1-42) sample alone. However, in SLN nanosystem it was observed a different scenario (Figure 19A). Hence, only SLN-RVG29 loaded with quercetin were able to inhibit peptide fibrillation when compared to Aβ(1-42) sample alone. This difference between SLN and NLC nanosystems can be attributed to their different crystalline structure and consequently their different capacity for accommodating quercetin in their lipid matrix. Actually, NLC have higher loading efficiency due to lattice defects that enhance quercetin entrapment, therefore better

preventing peptide fibrillation compared to SLN nanosystems. The mechanism that can explain the inhibition effect of some quercetin-formulations can be based on the ability to block some crucial regions in the amyloid-beta peptide responsible for monomers interaction [159-162]. Therefore, if these regions are blocked there will be no aggregation, so probably quercetin-formulations might interact with these domains, being efficient in the attenuation of Alzheimer's disease by inhibiting fibrils formation.

CONCLUDING REMARKS

Quercetin is a flavonol present in many vegetables and fruits. Generally, quercetin can be found in aglycone and glycoside forms, mainly in leaves. The absorption of this compound occurs in the large and small intestine where suffers glucuronidation, sulfatation and methylation in order to improve hydrophilicity. After metabolization, which occurs mainly in gut, it is distributed throughout the whole organism and is excreted by feces, urine, and also by exhalation of carbon dioxide. *In vivo* studies with animal models ensure the safety of quercetin. In fact, this compound can protect against cancer, cardiovascular diseases, chronic inflammation, oxidative stress and neurodegenerative diseases due to its radical scavenging and anti-inflammatory properties. However, its poor bioavailability is responsible for reducing the potential beneficial effects of this flavonoid and many types of nanocarriers have been developed to improve quercetin solubility and, at the same time, to deliver this compound specifically to their target places. All these studies manage to improve the bioavailability of quercetin allowing increasing its concentration in the desired places. By this way, it is clear that quercetin can become a promising compound if nanotechnology is employed as a tool to enhance its therapeutic efficacy.

In this work, the goal was to establish a new nanosystem capable of deliver quercetin to the brain. In the first step it was optimized the composition of lipid nanoparticles to create a stable vehicle. The nanoparticles (SLN and NLC) exhibited compatible sizes for brain application, lower than 250 nm, and zeta potential values higher than -30 mV, which confirm formulations stability. At the same time, these nanoparticles showed values of entrapment efficiency around 80-90%, which ensure that almost all quercetin was encapsulated inside lipid nanoparticles. After these preliminary steps, nanoparticles were functionalized with transferrin and RVG29 peptide. The functionalization of nanoparticles did not significantly change nanoparticles characteristics, like size, zeta potential or entrapment efficiency. Additionally, functionalization was confirmed by NMR and FTIR spectroscopic techniques, where the functional groups of ligands were identified in the respective spectra. The capacity of nanoparticles to protect quercetin from photodegradation was also studied. The results showed that only 10% of quercetin was degraded after 6 hours of UV light exposure when the compound was loaded inside nanoparticles, contrary to what

happens with free quercetin, where 55% was photodegraded. After this previous characterization, nanoparticles cytotoxicity was evaluated using the LDH assay on hCMEC/D3 cells. No relevant cytotoxic effects were observed even for the highest concentration tested, indicating that nanoparticles are safe to work at this range of concentrations. The next step consisted in testing the capacity of nanoparticles to enhance the permeation through hCMEC/D3 cell monolayers that mimetize the human BBB in a Transwell device. Nanoparticles functionalized with RVG29 showed better permeation capacity (1.5-fold higher) than nanoparticles with transferrin or without functionalization, probably taking part of the active expression of nicotinic acetylcholine receptors on brain endothelial cells. Finally, the ability of quercetin-loaded nanoparticles to promote neuroprotective effects was studied using an *in vitro* model of Alzheimer's disease with Aβ(1-42) peptide. It was demonstrated that quercetin-loaded nanoparticles, especially transferrin- and RVG29-functionalized NLC systems, were capable of inhibiting fibril formation, contradicting the aggregation effect of unloaded nanoparticles.

As a conclusion, it is possible to state that RVG29-functionalized nanoparticles were the most promising systems developed in this work, because they showed high quercetin entrapment and protection efficiencies, compatible sizes with brain applications, low cytotoxicity, capacity to enhance BBB permeability and the ability to inhibit amyloid-beta aggregation. Therefore, these nanosystems with RVG29, especially NLC-RVG29, seem to gather favorable characteristics that make them suitable carriers for quercetin, conferring protection and increasing the stability of this promising compound, while seem to be perfect candidates to deliver quercetin in the brain with greater potential to be used in Alzheimer's prevention or therapy.

REFERENCES

1. Harborne, J.B., *Flavonoids in the environment: structure-activity relationships.* Prog Clin Biol Res, 1988. **280**: p. 17-27.
2. Havsteen, B., *Flavonoids, a class of natural products of high pharmacological potency.* Biochem Pharmacol, 1983. **32**(7): p. 1141-8.
3. Formica, J.V. and W. Regelson, *Review of the biology of Quercetin and related bioflavonoids.* Food Chem Toxicol, 1995. **33**(12): p. 1061-80.
4. Murota, K. and J. Terao, *Antioxidative flavonoid quercetin: implication of its intestinal absorption and metabolism.* Arch Biochem Biophys, 2003. **417**(1): p. 12-7.
5. Wach, A., K. Pyrzyńska, and M. Biesaga, *Quercetin content in some food and herbal samples.* Food Chemistry, 2007. **100**(2): p. 699-704.
6. Harnly, J.M., et al., *Flavonoid content of U.S. fruits, vegetables, and nuts.* J Agric Food Chem, 2006. **54**(26): p. 9966-77.
7. Day, A.J. and G. Williamson, *Human metabolism of dietary quercetin glycosides.* Basic Life Sci, 1999. **66**: p. 415-34.
8. Bonaccorsi, P., et al., *Flavonol glucoside profile of southern Italian red onion (Allium cepa L.).* J Agric Food Chem, 2005. **53**(7): p. 2733-40.
9. Hakkinen, S.H., et al., *Content of the flavonols quercetin, myricetin, and kaempferol in 25 edible berries.* J Agric Food Chem, 1999. **47**(6): p. 2274-9.
10. Urbanek, M., et al., *On-line coupling of capillary isotachophoresis and capillary zone electrophoresis for the determination of flavonoids in methanolic extracts of Hypericum perforatum leaves or flowers.* J Chromatogr A, 2002. **958**(1-2): p. 261-71.
11. Sampson, L., et al., *Flavonol and flavone intakes in US health professionals.* J Am Diet Assoc, 2002. **102**(10): p. 1414-20.
12. Erlund, I., *Review of the flavonoids quercetin, hesperetin, and naringenin. Dietary sources, bioactivities, bioavailability, and epidemiology.* Nutrition Research. **24**(10): p. 851-874.
13. Brown, J.P., *A review of the genetic effects of naturally occurring flavonoids, anthraquinones and related compounds.* Mutat Res, 1980. **75**(3): p. 243-77.
14. Mendoza-Wilson, A.M. and D. Glossman-Mitnik, *CHIH-DFT study of the electronic properties and chemical reactivity of quercetin.* Journal of Molecular Structure: THEOCHEM, 2005. **716**(1–3): p. 67-72.
15. Codorniu-Hernández, E., et al., *Theoretical study of flavonoids and proline interactions. Aqueous and gas phases.* Journal of Molecular Structure: THEOCHEM, 2003. **623**(1–3): p. 63-73.
16. Kim, M.K., et al., *In vitro solubility, stability and permeability of novel quercetin–amino acid conjugates.* Bioorganic & Medicinal Chemistry, 2009. **17**(3): p. 1164-1171.
17. Althans, D., P. Schrader, and S. Enders, *Solubilisation of quercetin: Comparison of hyperbranched polymer and hydrogel.* Journal of Molecular Liquids, 2014. **196**: p. 86-93.
18. Gao, L., et al., *Preparation of a chemically stable quercetin formulation using nanosuspension technology.* International Journal of Pharmaceutics, 2011. **404**(1–2): p. 231-237.
19. Dall'Acqua, S., et al., *The photodegradation of quercetin: relation to oxidation.* Molecules, 2012. **17**(8): p. 8898-907.
20. Buchner, N., et al., *Effect of thermal processing on the flavonols rutin and quercetin.* Rapid Commun Mass Spectrom, 2006. **20**(21): p. 3229-35.
21. Murota, K. and J. Terao, *Antioxidative flavonoid quercetin: implication of its intestinal absorption and metabolism.* Archives of Biochemistry and Biophysics, 2003. **417**(1): p. 12-17.

22. Chen, X., et al., *Pharmacokinetics and modeling of quercetin and metabolites.* Pharm Res, 2005. **22**(6): p. 892-901.
23. Walle, T., U.K. Walle, and P.V. Halushka, *Carbon dioxide is the major metabolite of quercetin in humans.* J Nutr, 2001. **131**(10): p. 2648-52.
24. Petri, N., et al., *Absorption/metabolism of sulforaphane and quercetin, and regulation of phase II enzymes, in human jejunum in vivo.* Drug Metab Dispos, 2003. **31**(6): p. 805-13.
25. Rechner, A.R., et al., *The metabolic fate of dietary polyphenols in humans.* Free Radic Biol Med, 2002. **33**(2): p. 220-35.
26. Murota, K. and J. Terao, *Quercetin appears in the lymph of unanesthetized rats as its phase II metabolites after administered into the stomach.* FEBS Lett, 2005. **579**(24): p. 5343-6.
27. Graf, B.A., et al., *Rat gastrointestinal tissues metabolize quercetin.* J Nutr, 2006. **136**(1): p. 39-44.
28. Crespy, V., et al., *Part of quercetin absorbed in the small intestine is conjugated and further secreted in the intestinal lumen.* Am J Physiol, 1999. **277**(1 Pt 1): p. G120-6.
29. O'Leary, K.A., et al., *Metabolism of quercetin-7- and quercetin-3-glucuronides by an in vitro hepatic model: the role of human beta-glucuronidase, sulfotransferase, catechol-O-methyltransferase and multi-resistant protein 2 (MRP2) in flavonoid metabolism.* Biochem Pharmacol, 2003. **65**(3): p. 479-91.
30. De Santi, C., et al., *Methylation of quercetin and fisetin, flavonoids widely distributed in edible vegetables, fruits and wine, by human liver.* Int J Clin Pharmacol Ther, 2002. **40**(5): p. 207-12.
31. Boulton, D.W., U.K. Walle, and T. Walle, *Extensive binding of the bioflavonoid quercetin to human plasma proteins.* J Pharm Pharmacol, 1998. **50**(2): p. 243-9.
32. Moon, J.H., et al., *Accumulation of quercetin conjugates in blood plasma after the short-term ingestion of onion by women.* Am J Physiol Regul Integr Comp Physiol, 2000. **279**(2): p. R461-7.
33. de Boer, V.C., et al., *Tissue distribution of quercetin in rats and pigs.* J Nutr, 2005. **135**(7): p. 1718-25.
34. Abrahamse, S.L., W.J. Kloots, and J.M.M. van Amelsvoort, *Absorption, distribution, and secretion of epicatechin and quercetin in the rat.* Nutrition Research, 2005. **25**(3): p. 305-317.
35. Gugler, R., M. Leschik, and H.J. Dengler, *Disposition of quercetin in man after single oral and intravenous doses.* Eur J Clin Pharmacol, 1975. **9**(2-3): p. 229-34.
36. de Vries, J.H., et al., *Plasma concentrations and urinary excretion of the antioxidant flavonols quercetin and kaempferol as biomarkers for dietary intake.* Am J Clin Nutr, 1998. **68**(1): p. 60-5.
37. Young, J.F., et al., *Effect of fruit juice intake on urinary quercetin excretion and biomarkers of antioxidative status.* Am J Clin Nutr, 1999. **69**(1): p. 87-94.
38. Ueno, I., N. Nakano, and I. Hirono, *Metabolic fate of [14C] quercetin in the ACI rat.* Jpn J Exp Med, 1983. **53**(1): p. 41-50.
39. Bjeldanes, L.F. and G.W. Chang, *Mutagenic activity of quercetin and related compounds.* Science, 1977. **197**(4303): p. 577-8.
40. Hardigree, A.A. and J.L. Epler, *Comparative mutagenesis of plant flavonoids in microbial systems.* Mutat Res, 1978. **58**(2-3): p. 231-9.
41. Brown, J.P. and P.S. Dietrich, *Mutagenicity of plant flavonols in the Salmonella/mammalian microsome test: activation of flavonol glycosides by mixed glycosidases from rat cecal bacteria and other sources.* Mutat Res, 1979. **66**(3): p. 223-40.
42. Rueff, J., et al., *Oxygen species and the genotoxicity of quercetin.* Mutat Res, 1992. **265**(1): p. 75-81.

43. Yoshida, M.A., et al., *Cytogenetic Effects of Quercetin on Cultured Mammalian Cells.* Proceedings of the Japan Academy, Series B, 1980. **56**(7): p. 443-447.
44. Meltz, M.L. and J.T. MacGregor, *Activity of the plant flavanol quercetin in the mouse lymphoma L5178Y TK+/- mutation, DNA single-strand break, and Balb/c 3T3 chemical transformation assays.* Mutat Res, 1981. **88**(3): p. 317-24.
45. Cierniak, A., M. Papiez, and M. Kapiszewska, *Modulatory effect of quercetin on DNA damage, induced by etoposide in bone marrow cells and on changes in the activity of antioxidant enzymes in rats.* Rocz Akad Med Bialymst, 2004. **49 Suppl 1**: p. 167-9.
46. Ngomuo, A.J. and R.S. Jones, *Genotoxicity studies of quercetin and shikimate in vivo in the bone marrow of mice and gastric mucosal cells of rats.* Vet Hum Toxicol, 1996. **38**(3): p. 176-80.
47. Takanashi, H., et al., *CARCINOGENICITY TEST OF QUERCETIN AND KAEMPFEROL IN RATS BY ORAL ADMINISTRATION.* Journal of Food Safety, 1983. **5**(2): p. 55-60.
48. Hosaka, S. and I. Hirono, *Carcinogenicity test of quercetin by pulmonary-adenoma bioassay in strain A mice.* Gan, 1981. **72**(2): p. 327-8.
49. Davis, J.M., E.A. Murphy, and M.D. Carmichael, *Effects of the dietary flavonoid quercetin upon performance and health.* Curr Sports Med Rep, 2009. **8**(4): p. 206-13.
50. Murakami, A., H. Ashida, and J. Terao, *Multitargeted cancer prevention by quercetin.* Cancer Lett, 2008. **269**(2): p. 315-25.
51. Ashida, H., et al., *Flavones and flavonols at dietary levels inhibit a transformation of aryl hydrocarbon receptor induced by dioxin.* FEBS Letters, 2000. **476**(3): p. 213-217.
52. Chen, W., et al., *Induction of death receptor 5 and suppression of survivin contribute to sensitization of TRAIL-induced cytotoxicity by quercetin in non-small cell lung cancer cells.* Carcinogenesis, 2007. **28**(10): p. 2114-21.
53. Kim, W.K., et al., *Quercetin decreases the expression of ErbB2 and ErbB3 proteins in HT-29 human colon cancer cells.* The Journal of Nutritional Biochemistry, 2005. **16**(3): p. 155-162.
54. Xing, N., et al., *Quercetin inhibits the expression and function of the androgen receptor in LNCaP prostate cancer cells.* Carcinogenesis, 2001. **22**(3): p. 409-14.
55. Galindo, P., et al., *Different cardiovascular protective effects of quercetin administered orally or intraperitoneally in spontaneously hypertensive rats.* Food Funct, 2012. **3**(6): p. 643-50.
56. Sanchez, M., et al., *Quercetin downregulates NADPH oxidase, increases eNOS activity and prevents endothelial dysfunction in spontaneously hypertensive rats.* J Hypertens, 2006. **24**(1): p. 75-84.
57. Booyse, F.M., et al., *Mechanism by which alcohol and wine polyphenols affect coronary heart disease risk.* Ann Epidemiol, 2007. **17**(5 Suppl): p. S24-31.
58. Edwards, R.L., et al., *Quercetin reduces blood pressure in hypertensive subjects.* J Nutr, 2007. **137**(11): p. 2405-11.
59. Mamani-Matsuda, M., et al., *Therapeutic and preventive properties of quercetin in experimental arthritis correlate with decreased macrophage inflammatory mediators.* Biochem Pharmacol, 2006. **72**(10): p. 1304-10.
60. Rogerio, A.P., et al., *Anti-inflammatory activity of quercetin and isoquercitrin in experimental murine allergic asthma.* Inflamm Res, 2007. **56**(10): p. 402-8.
61. Min, Y.D., et al., *Quercetin inhibits expression of inflammatory cytokines through attenuation of NF-kappaB and p38 MAPK in HMC-1 human mast cell line.* Inflamm Res, 2007. **56**(5): p. 210-5.
62. Kimata, et al., *Effects of luteolin, quercetin and baicalein on immunoglobulin E-mediated mediator release from human cultured mast cells.* Clinical & Experimental Allergy, 2000. **30**(4): p. 501-508.

63. Afanas'ev, I.B., et al., *Chelating and free radical scavenging mechanisms of inhibitory action of rutin and quercetin in lipid peroxidation.* Biochem Pharmacol, 1989. **38**(11): p. 1763-9.
64. van Acker, S.A., et al., *Influence of iron chelation on the antioxidant activity of flavonoids.* Biochem Pharmacol, 1998. **56**(8): p. 935-43.
65. Harwood, M., et al., *A critical review of the data related to the safety of quercetin and lack of evidence of in vivo toxicity, including lack of genotoxic/carcinogenic properties.* Food Chem Toxicol, 2007. **45**(11): p. 2179-205.
66. Kim, G.N. and H.D. Jang, *Protective mechanism of quercetin and rutin using glutathione metabolism on HO-induced oxidative stress in HepG2 cells.* Ann N Y Acad Sci, 2009. **1171**: p. 530-7.
67. Chen, J.C., et al., *Inhibition of iNOS gene expression by quercetin is mediated by the inhibition of IkappaB kinase, nuclear factor-kappa B and STAT1, and depends on heme oxygenase-1 induction in mouse BV-2 microglia.* Eur J Pharmacol, 2005. **521**(1-3): p. 9-20.
68. Heo, H.J. and C.Y. Lee, *Protective effects of quercetin and vitamin C against oxidative stress-induced neurodegeneration.* J Agric Food Chem, 2004. **52**(25): p. 7514-7.
69. Zhang, Z.J., et al., *Quercetin exerts a neuroprotective effect through inhibition of the iNOS/NO system and pro-inflammation gene expression in PC12 cells and in zebrafish.* Int J Mol Med, 2011. **27**(2): p. 195-203.
70. Dok-Go, H., et al., *Neuroprotective effects of antioxidative flavonoids, quercetin, (+)-dihydroquercetin and quercetin 3-methyl ether, isolated from Opuntia ficus-indica var. saboten.* Brain Res, 2003. **965**(1-2): p. 130-6.
71. Sagara, Y., J. Vanhnasy, and P. Maher, *Induction of PC12 cell differentiation by flavonoids is dependent upon extracellular signal-regulated kinase activation.* J Neurochem, 2004. **90**(5): p. 1144-55.
72. Ansari, M.A., et al., *Protective effect of quercetin in primary neurons against Abeta(1-42): relevance to Alzheimer's disease.* J Nutr Biochem, 2009. **20**(4): p. 269-75.
73. Kim, H., et al., *Effects of naturally occurring compounds on fibril formation and oxidative stress of beta-amyloid.* J Agric Food Chem, 2005. **53**(22): p. 8537-41.
74. Davis, J.M., et al., *Quercetin increases brain and muscle mitochondrial biogenesis and exercise tolerance.* Am J Physiol Regul Integr Comp Physiol, 2009. **296**(4): p. R1071-7.
75. Sharma, V., et al., *Modulation of interleukin-1beta mediated inflammatory response in human astrocytes by flavonoids: implications in neuroprotection.* Brain Res Bull, 2007. **73**(1-3): p. 55-63.
76. Priprem, A., et al., *Anxiety and cognitive effects of quercetin liposomes in rats.* Nanomedicine, 2008. **4**(1): p. 70-8.
77. Shaji, J. and S. Iyer, *Preparation, optimization and in-vivo hepatoprotective evaluation of quercetin liposomes.* Int J Curr Pharm Res, 2012. **4**(2): p. 24-32.
78. Yuan, Z.P., et al., *Liposomal quercetin efficiently suppresses growth of solid tumors in murine models.* Clin Cancer Res, 2006. **12**(10): p. 3193-9.
79. Long, Q., et al., *Induction of apoptosis and inhibition of angiogenesis by PEGylated liposomal quercetin in both cisplatin-sensitive and cisplatin-resistant ovarian cancers.* J Biomed Nanotechnol, 2013. **9**(6): p. 965-75.
80. Wong, M.Y. and G.N. Chiu, *Liposome formulation of co-encapsulated vincristine and quercetin enhanced antitumor activity in a trastuzumab-insensitive breast tumor xenograft model.* Nanomedicine, 2011. **7**(6): p. 834-40.
81. Goniotaki, M., et al., *Encapsulation of naturally occurring flavonoids into liposomes: physicochemical properties and biological activity against human cancer cell lines.* J Pharm Pharmacol, 2004. **56**(10): p. 1217-24.
82. Li, H., et al., *Enhancement of gastrointestinal absorption of quercetin by solid lipid nanoparticles.* J Control Release, 2009. **133**(3): p. 238-44.

83. Chen-yu, G., et al., *Development of a quercetin-loaded nanostructured lipid carrier formulation for topical delivery.* Int J Pharm, 2012. **430**(1-2): p. 292-8.
84. Bose, S., et al., *Formulation optimization and topical delivery of quercetin from solid lipid based nanosystems.* Int J Pharm, 2013. **441**(1-2): p. 56-66.
85. Sun, M., et al., *Quercetin-nanostructured lipid carriers: characteristics and anti-breast cancer activities in vitro.* Colloids Surf B Biointerfaces, 2014. **113**: p. 15-24.
86. Dhawan, S., R. Kapil, and B. Singh, *Formulation development and systematic optimization of solid lipid nanoparticles of quercetin for improved brain delivery.* J Pharm Pharmacol, 2011. **63**(3): p. 342-51.
87. Kumari, A., et al., *Development of biodegradable nanoparticles for delivery of quercetin.* Colloids Surf B Biointerfaces, 2010. **80**(2): p. 184-92.
88. Khoee, S. and R. Rahmatolahzadeh, *Synthesis and characterization of pH-responsive and folated nanoparticles based on self-assembled brush-like PLGA/PEG/AEMA copolymer with targeted cancer therapy properties: A comprehensive kinetic study.* Eur J Med Chem, 2012. **50**: p. 416-27.
89. El-Gogary, R.I., et al., *Polyethylene glycol conjugated polymeric nanocapsules for targeted delivery of quercetin to folate-expressing cancer cells in vitro and in vivo.* ACS Nano, 2014. **8**(2): p. 1384-401.
90. Bishayee, K., A.R. Khuda-Bukhsh, and S.O. Huh, *PLGA-Loaded Gold-Nanoparticles Precipitated with Quercetin Downregulate HDAC-Akt Activities Controlling Proliferation and Activate p53-ROS Crosstalk to Induce Apoptosis in Hepatocarcinoma Cells.* Mol Cells, 2015. **38**(6): p. 518-27.
91. Pandey, S.K., et al., *Anti-cancer evaluation of quercetin embedded PLA nanoparticles synthesized by emulsified nanoprecipitation.* Int J Biol Macromol, 2015. **75**: p. 521-9.
92. Sun, D., et al., *Design of PLGA-functionalized quercetin nanoparticles for potential use in Alzheimer's disease.* Colloids Surf B Biointerfaces, 2016. **148**: p. 116-129.
93. Suksiriworapong, J., et al., *Comparison of poly(ε-caprolactone) chain lengths of poly(ε-caprolactone)-co-d-α-tocopheryl-poly(ethylene glycol) 1000 succinate nanoparticles for enhancement of quercetin delivery to SKBR3 breast cancer cells.* European Journal of Pharmaceutics and Biopharmaceutics, 2016. **101**: p. 15-24.
94. Zhu, X., et al., *The effects of quercetin-loaded PLGA-TPGS nanoparticles on ultraviolet B-induced skin damages in vivo.* Nanomedicine, 2016. **12**(3): p. 623-32.
95. Barreto, A.C.H., et al., *Magnetic nanoparticles for a new drug delivery system to control quercetin releasing for cancer chemotherapy.* Journal of Nanoparticle Research, 2011. **13**(12): p. 6545-6553.
96. Verma, N.K., et al., *Magnetic core-shell nanoparticles for drug delivery by nebulization.* J Nanobiotechnology, 2013. **11**: p. 1.
97. Kumar, S.R., et al., *Quercetin conjugated superparamagnetic magnetite nanoparticles for in-vitro analysis of breast cancer cell lines for chemotherapy applications.* J Colloid Interface Sci, 2014. **436**: p. 234-42.
98. Akal, Z.Ü., L. Alpsoy, and A. Baykal, *Superparamagnetic iron oxide conjugated with folic acid and carboxylated quercetin for chemotherapy applications.* Ceramics International, 2016. **42**(7): p. 9065-9072.
99. Sapino, S., et al., *Mesoporous silica as topical nanocarriers for quercetin: characterization and in vitro studies.* Eur J Pharm Biopharm, 2015. **89**: p. 116-25.
100. Sarkar, A., et al., *Targeted delivery of quercetin loaded mesoporous silica nanoparticles to the breast cancer cells.* Biochim Biophys Acta, 2016. **1860**(10): p. 2065-75.
101. Jullian, C., et al., *Complexation of quercetin with three kinds of cyclodextrins: an antioxidant study.* Spectrochim Acta A Mol Biomol Spectrosc, 2007. **67**(1): p. 230-4.
102. Liu, M., et al., *Inclusion complexes of quercetin with three β-cyclodextrins derivatives at physiological pH: Spectroscopic study and antioxidant activity.* Spectrochimica Acta Part A: Molecular and Biomolecular Spectroscopy, 2013. **115**: p. 854-860.

103. Aytac, Z., et al., *Quercetin/β-cyclodextrin inclusion complex embedded nanofibres: Slow release and high solubility.* Food Chemistry, 2016. **197, Part A**: p. 864-871.
104. Kale, R., et al., *Decreased B16F10 melanoma growth and impaired tumour vascularization in BDF1 mice with quercetin-cyclodextrin binary system.* J Pharm Pharmacol, 2006. **58**(10): p. 1351-8.
105. Akbarzadeh, A., et al., *Liposome: classification, preparation, and applications.* Nanoscale Res Lett, 2013. **8**(1): p. 102.
106. Immordino, M.L., F. Dosio, and L. Cattel, *Stealth liposomes: review of the basic science, rationale, and clinical applications, existing and potential.* Int J Nanomedicine, 2006. **1**(3): p. 297-315.
107. Phachonpai, W., *Neuroprotective Effect of Quercetin Encapsulated Liposomes: A Novel Therapeutic Strategy against Alzheimer’s Disease*, ed. J. Wattanathorn, et al. 2010: Science Publications.
108. Weber, S., A. Zimmer, and J. Pardeike, *Solid Lipid Nanoparticles (SLN) and Nanostructured Lipid Carriers (NLC) for pulmonary application: a review of the state of the art.* Eur J Pharm Biopharm, 2014. **86**(1): p. 7-22.
109. Wissing, S.A., O. Kayser, and R.H. Muller, *Solid lipid nanoparticles for parenteral drug delivery.* Adv Drug Deliv Rev, 2004. **56**(9): p. 1257-72.
110. Mehnert, W. and K. Mäder, *Solid lipid nanoparticles: Production, characterization and applications.* Advanced Drug Delivery Reviews, 2001. **47**(2–3): p. 165-196.
111. des Rieux, A., et al., *Nanoparticles as potential oral delivery systems of proteins and vaccines: a mechanistic approach.* J Control Release, 2006. **116**(1): p. 1-27.
112. Alexiou, C., et al., *Targeting cancer cells: magnetic nanoparticles as drug carriers.* European Biophysics Journal, 2006. **35**(5): p. 446-450.
113. Lu, A.H., E.L. Salabas, and F. Schuth, *Magnetic nanoparticles: synthesis, protection, functionalization, and application.* Angew Chem Int Ed Engl, 2007. **46**(8): p. 1222-44.
114. Cauda, V., et al., *Tuning drug uptake and release rates through different morphologies and pore diameters of confined mesoporous silica.* Microporous and Mesoporous Materials, 2009. **118**(1–3): p. 435-442.
115. Vallet-Regi, M., F. Balas, and D. Arcos, *Mesoporous materials for drug delivery.* Angew Chem Int Ed Engl, 2007. **46**(40): p. 7548-58.
116. Manzano, M., M. Colilla, and M. Vallet-Regi, *Drug delivery from ordered mesoporous matrices.* Expert Opin Drug Deliv, 2009. **6**(12): p. 1383-400.
117. Di Pasqua, A.J., et al., *Cytotoxicity of mesoporous silica nanomaterials.* Journal of Inorganic Biochemistry, 2008. **102**(7): p. 1416-1423.
118. Lu, J., et al., *Biocompatibility, biodistribution, and drug-delivery efficiency of mesoporous silica nanoparticles for cancer therapy in animals.* Small, 2010. **6**(16): p. 1794-805.
119. Wang, W., et al., *The biological activities, chemical stability, metabolism and delivery systems of quercetin: A review.* Trends in Food Science & Technology, 2016. **56**: p. 21-38.
120. Lucas-Abellán, C., et al., *Cyclodextrins as resveratrol carrier system.* Food Chemistry, 2007. **104**(1): p. 39-44.
121. Kawabata, K., R. Mukai, and A. Ishisaka, *Quercetin and related polyphenols: new insights and implications for their bioactivity and bioavailability.* Food Funct, 2015. **6**(5): p. 1399-417.
122. Boots, A.W., G.R. Haenen, and A. Bast, *Health effects of quercetin: from antioxidant to nutraceutical.* Eur J Pharmacol, 2008. **585**(2-3): p. 325-37.
123. Gomes, M.J., et al., *Tailoring Lipid and Polymeric Nanoparticles as siRNA Carriers towards the Blood-Brain Barrier - from Targeting to Safe Administration.* J Neuroimmune Pharmacol, 2017. **12**(1): p. 107-119.

124. Oller-Salvia, B., et al., *Blood-brain barrier shuttle peptides: an emerging paradigm for brain delivery.* Chem Soc Rev, 2016. **45**(17): p. 4690-707.
125. Lajoie, J.M. and E.V. Shusta, *Targeting receptor-mediated transport for delivery of biologics across the blood-brain barrier.* Annual review of pharmacology and toxicology, 2015. **55**: p. 613-631.
126. Neves, A.R., et al., *Novel resveratrol nanodelivery systems based on lipid nanoparticles to enhance its oral bioavailability.* Int J Nanomedicine, 2013. **8**: p. 177-87.
127. Gastaldi, L., et al., *Solid lipid nanoparticles as vehicles of drugs to the brain: current state of the art.* Eur J Pharm Biopharm, 2014. **87**(3): p. 433-44.
128. Neves, A.R., J.F. Queiroz, and S. Reis, *Brain-targeted delivery of resveratrol using solid lipid nanoparticles functionalized with apolipoprotein E.* J Nanobiotechnology, 2016. **14**: p. 27.
129. Weksler, B., I.A. Romero, and P.O. Couraud, *The hCMEC/D3 cell line as a model of the human blood brain barrier.* Fluids Barriers CNS, 2013. **10**(1): p. 16.
130. Weksler, B.B., et al., *Blood-brain barrier-specific properties of a human adult brain endothelial cell line.* FASEB J, 2005. **19**(13): p. 1872-4.
131. Poller, B., et al., *The human brain endothelial cell line hCMEC/D3 as a human blood-brain barrier model for drug transport studies.* J Neurochem, 2008. **107**(5): p. 1358-68.
132. Soto, C., et al., *Fibrillogenesis of synthetic amyloid-beta peptides is dependent on their initial secondary structure.* Neuroscience Letters, 1995. **200**(2): p. 105-8.
133. Sabate, R. and J. Estelrich, *Stimulatory and inhibitory effects of alkyl bromide surfactants on beta-amyloid fibrillogenesis.* Langmuir, 2005. **21**(15): p. 6944-9.
134. Nilsson, M.R., *Techniques to study amyloid fibril formation in vitro.* Methods, 2004. **34**(1): p. 151-60.
135. Rocha, S., et al., *Design and biological activity of beta-sheet breaker peptide conjugates.* Biochemical and Biophysical Research Communications, 2009. **380**(2): p. 397-401.
136. Jameson, L.P., N.W. Smith, and S.V. Dzyuba, *Dye-binding assays for evaluation of the effects of small molecule inhibitors on amyloid (abeta) self-assembly.* ACS Chem Neurosci, 2012. **3**(11): p. 807-19.
137. LeVine, H., 3rd, *Thioflavine T interaction with synthetic Alzheimer's disease beta-amyloid peptides: detection of amyloid aggregation in solution.* Protein Sci, 1993. **2**(3): p. 404-10.
138. Lopes-de-Araujo, J., et al., *Oxaprozin-Loaded Lipid Nanoparticles towards Overcoming NSAIDs Side-Effects.* Pharm Res, 2016. **33**(2): p. 301-14.
139. Shah, N., et al., *Paclitaxel-loaded PLGA nanoparticles surface modified with transferrin and Pluronic((R))P85, an in vitro cell line and in vivo biodistribution studies on rat model.* J Drug Target, 2009. **17**(7): p. 533-42.
140. Liu, K., et al., *Self-assembled targeted nanoparticles based on transferrin-modified eight-arm-polyethylene glycol–dihydroartemisinin conjugate.* Scientific Reports, 2016. **6**: p. 29461.
141. Yan, Z., et al., *Tumor-penetrating peptide mediation: an effective strategy for improving the transport of liposomes in tumor tissue.* Mol Pharm, 2014. **11**(1): p. 218-25.
142. Liu, Y., et al., *Brain-targeting gene delivery and cellular internalization mechanisms for modified rabies virus glycoprotein RVG29 nanoparticles.* Biomaterials, 2009. **30**(25): p. 4195-202.
143. Wei, X., et al., *Retro-inverso isomer of Angiopep-2: a stable d-peptide ligand inspires brain-targeted drug delivery.* Mol Pharm, 2014. **11**(10): p. 3261-8.
144. Baker, M.J., et al., *Using Fourier transform IR spectroscopy to analyze biological materials.* Nature protocols, 2014. **9**(8): p. 1771-1791.

145. Baker, M.J., et al., *Developing and understanding biofluid vibrational spectroscopy: a critical review.* Chemical Society Reviews, 2016. **45**(7): p. 1803-1818.
146. Gaumet, M., et al., *Nanoparticles for drug delivery: the need for precision in reporting particle size parameters.* Eur J Pharm Biopharm, 2008. **69**(1): p. 1-9.
147. Bhattacharjee, S., *DLS and zeta potential - What they are and what they are not?* J Control Release, 2016.
148. Radomski, A., et al., *Nanoparticle-induced platelet aggregation and vascular thrombosis.* British Journal of Pharmacology, 2005. **146**(6): p. 882-893.
149. Naseri, N., H. Valizadeh, and P. Zakeri-Milani, *Solid Lipid Nanoparticles and Nanostructured Lipid Carriers: Structure, Preparation and Application.* Advanced Pharmaceutical Bulletin, 2015. **5**(3): p. 305-313.
150. Freitas, C. and R.H. Muller, *Correlation between long-term stability of solid lipid nanoparticles (SLN) and crystallinity of the lipid phase.* Eur J Pharm Biopharm, 1999. **47**(2): p. 125-32.
151. Burd, J.F. and M. Usategui-Gomez, *A colorimetric assay for serum lactate dehydrogenase.* Clinica Chimica Acta, 1973. **46**(3): p. 223-227.
152. Korzeniewski, C. and D.M. Callewaert, *An enzyme-release assay for natural cytotoxicity.* J Immunol Methods, 1983. **64**(3): p. 313-20.
153. Loureiro, J.A., et al., *Immunoliposomes doubly targeted to transferrin receptor and to α-synuclein.* Future Science OA, 2015. **1**(4): p. FSO71.
154. Hawkins, B.T., R.D. Egleton, and T.P. Davis, *Modulation of cerebral microvascular permeability by endothelial nicotinic acetylcholine receptors.* Am J Physiol Heart Circ Physiol, 2005. **289**(1): p. H212-9.
155. Phoolcharoen, W., et al., *Enhanced transport of plant-produced rabies single-chain antibody-RVG peptide fusion protein across an in cellulo blood-brain barrier device.* Plant Biotechnol J, 2017. **15**(10): p. 1331-1339.
156. Loureiro, J.A., S. Rocha, and C. Pereira Mdo, *Charged surfactants induce a non-fibrillar aggregation pathway of amyloid-beta peptide.* J Pept Sci, 2013. **19**(9): p. 581-7.
157. Loureiro, J.A., et al., *Dual ligand immunoliposomes for drug delivery to the brain.* Colloids Surf B Biointerfaces, 2015. **134**: p. 213-9.
158. Loureiro, J.A., et al., *Resveratrol and Grape Extract-loaded Solid Lipid Nanoparticles for the Treatment of Alzheimer's Disease.* Molecules, 2017. **22**(2).
159. Petkova, A.T., et al., *A structural model for Alzheimer's beta -amyloid fibrils based on experimental constraints from solid state NMR.* Proc Natl Acad Sci U S A, 2002. **99**(26): p. 16742-7.
160. Pike, C.J., et al., *Structure-activity analyses of beta-amyloid peptides: contributions of the beta 25-35 region to aggregation and neurotoxicity.* J Neurochem, 1995. **64**(1): p. 253-65.
161. Torok, M., et al., *Structural and dynamic features of Alzheimer's Abeta peptide in amyloid fibrils studied by site-directed spin labeling.* J Biol Chem, 2002. **277**(43): p. 40810-5.
162. Antzutkin, O.N., J.J. Balbach, and R. Tycko, *Site-specific identification of non-beta-strand conformations in Alzheimer's beta-amyloid fibrils by solid-state NMR.* Biophys J, 2003. **84**(5): p. 3326-35.